

Discovery and Synthesis of GS-5734, a Phosphoramidate Prodrug of a Pyrrolo[2,1-*f*][triazin-4-amino] Adenine C-Nucleoside for the Treatment of Ebola and Emerging Viruses

Dustin Siegel¹, Hon C. Hui¹, Edward Doerffler¹, Michael O. Clarke¹, Kwon Chun¹, Lijun Zhang¹, Sean Neville¹, Ernest Carra¹, Willard Lew¹, Bruce Ross¹, Queenie Wang¹, Lydia Wolfe¹, Robert Jordan¹, Veronica Soloveva², John Knox¹, Jason Perry¹, Michel Perron¹, Kirsten M. Stray¹, Ona Baraskaus¹, Joy Y. Feng¹, Yili Xu¹, Gary Lee¹, Arnold L. Rheingold³, Adrian S. Ray¹, Roy Bannister¹, Robert Strickley¹, Swami Swaminathan¹, William A. Lee¹, Sina Bavari², Tomas Cihlar¹, Michael K. Lo⁴, Travis K. Warren², and Richard L. Mackman^{1*}

¹Gilead Sciences, Inc. Foster City, California, USA.

²United States Army Medical Research Institute of Infectious Diseases (USAMRIID), Frederick, Maryland, USA. § USAMRIID Therapeutic Development Center (TDC), Frederick, Maryland, USA.

³UC San Diego, San Diego, California, USA

⁴Centers for Disease Control and Prevention, Atlanta, Georgia, USA.

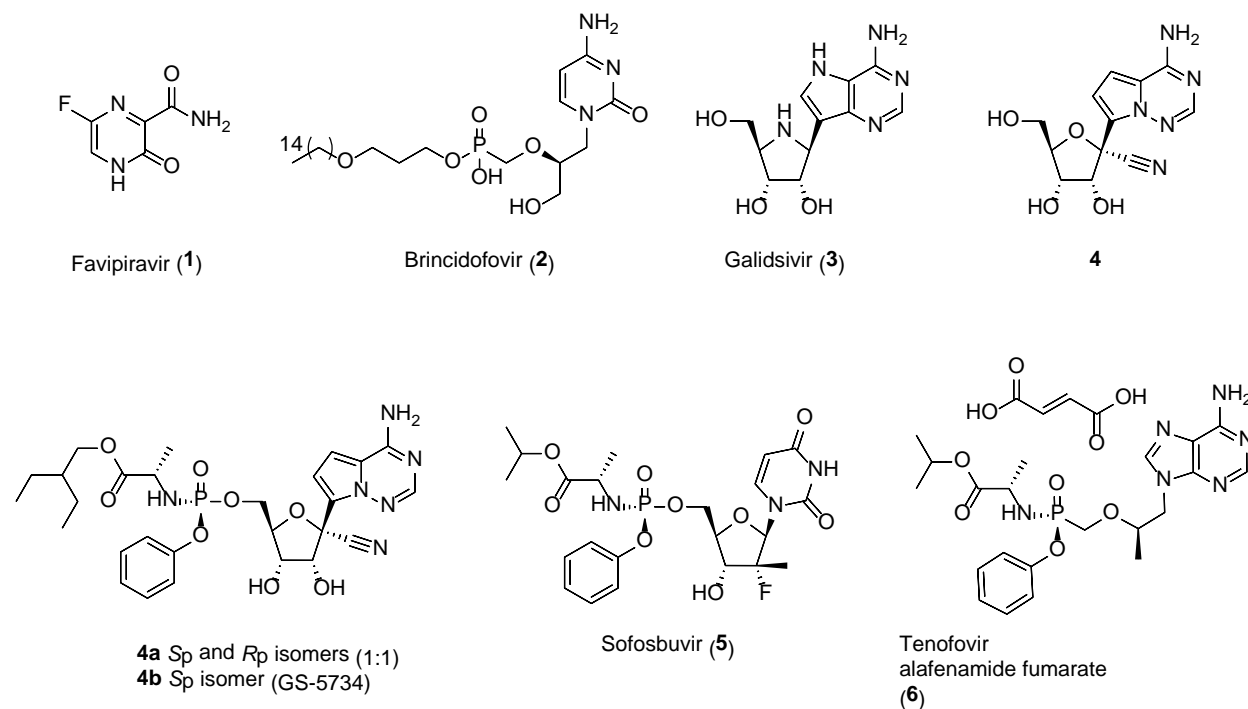
ABSTRACT

The recent Ebola outbreak in West Africa was the largest recorded in history with over 28,000 cases confirmed in Guinea, Liberia, and Sierra Leone resulting in >11,000 deaths including >500 healthcare workers. This international crisis demonstrated the urgent need for a safe, effective and readily available treatment of Ebola infection. Multiple promising small molecule drugs and biologics were rapidly pushed into clinical trials, including several nucleoside based therapeutics. From our nucleoside library, a focused screening effort identified a 1'-CN modified C-nucleoside **4** and a phosphoramidate prodrug mixture **4a**, that demonstrated potent anti-EBOV activity across multiple viral variants and cell lines in vitro ($EC_{50} < 170$ nM). Structure activity relationships established that the 1'-CN group and C-linked nucleobase were critical both for optimal anti-EBOV potency and anti-viral selectivity versus host polymerases. From a suite of phosphoramidate prodrugs the 2-ethylbutyl alaninyl monophosphoramidate prodrug Sp isomer GS-5734, **4b** was identified with anti-EBOV $EC_{50} < 100$ nM and broad spectrum activity toward several other families of RNA viruses. The Sp isomer was confirmed by X-Ray and the development of a robust and diastereoselective synthesis provided sufficient quantities of **4b** to enable preclinical efficacy and safety studies. In a non-human primate EBOV challenge model, once-daily, 10 mg/kg i.v. treatment with **4b** on days 3-14 post infection had a significant effect on viremia and mortality resulting in 100% survival of infected treated animals [Nature **2016**, 531, 381-385]. Phase 1 studies with **4b** in normal human volunteers have been completed, and the compound has been provided to two patients with confirmed Ebola infection under compassionate use protocol. A phase 2 study (PREVAIL IV) is currently enrolling and will evaluate the effect of **4b** on viral shedding from sanctuary sites in Ebola survivors.

Discovery and Synthesis of GS-5734, a Phosphoramidate Prodrug of a Pyrrolo[2,1-*f*][triazin-4-amino] Adenine C-Nucleoside for the Treatment of Ebola and Emerging Viruses

Ebola Virus Disease (EVD) was first documented 40 years ago during an outbreak of infectious hemorrhagic fever in Northern Zaire (current Democratic Republic of Congo). More than 20 intermittent outbreaks have occurred since then, but the most recent outbreak in West Africa spanning 2014-2016 has been the largest recorded in history and presented an international public health emergency.¹ Over 28,000 cases were confirmed in Guinea, Liberia, and Sierra Leone resulting in >11,000 deaths including >500 healthcare workers, which severely strained the local medical infrastructure.² In survivors, the Ebola virus (EBOV) can persist in bodily fluids for months after the onset of acute infection potentially leading to EVD-related sequelae and viral recrudescence.³ While rare, secondary transmission has been documented to occur through sexual intercourse implicating persistent virus in genital secretions.⁴ Despite the end of the current outbreak, the potential for equally devastating future outbreaks, together with the persistent virus observed in survivors makes the development of a safe, effective and readily available treatment option for EVD a high priority.

EBOV, a member of the *Filoviridae* family, is a single-stranded, negative-sense, non-segmented RNA virus that is the causative agent of EVD. Other *filoviridae* family members include Marburg, Sudan, and Bundibugyo viruses, which have all been responsible for outbreaks associated with high mortality rates in sub-Saharan Africa.^{5,6} Over the course of the recent West African EVD outbreak, several direct acting anti-Ebola agents including monoclonal antibodies (ZMappTM),⁷ interfering-RNAs (TKM-Ebola,^{8,9} AVI-7537¹⁰), and small molecule nucleoside(tide) antivirals such as favipiravir (**1**),¹¹⁻¹³ and brincidofovir (**2**)¹⁴ have been evaluated in early clinical trials (Figure 1). More recently another nucleoside analogue, galidesivir (**3**, BCX4430), has entered clinical development.¹⁵ These developments are encouraging but to date, none of these potential therapeutics have established robust clinical efficacy for the treatment of acute infection or the viral persistence and sequelae. Several vaccines have shown strong promise for preventing EBOV infection, but the breadth and durability of protection they can afford has yet to be established.¹⁶

Figure 1. Structures of antiviral nucleosides, nucleoside phosphonates and their prodrugs.

Prior to the Ebola outbreak, we had embarked on a strategic initiative aimed at evaluating the potential of nucleoside analogs for the treatment of selected emerging viruses. A library of ~1000 diverse nucleoside and nucleoside phosphonate analogs was harnessed from over two decades of research across multiple antiviral programs. In collaboration with the Center for Disease Control and Prevention (CDC), and the United States Army Medical Research Institute of Infectious Diseases (USAMRIID), selected compounds from the library were screened against EBOV and identified parent **4** and a potent monophosphate prodrug mixture that contained the *Sp* isomer GS-5734 (**4b**). This report describes in detail the structure activity relationships of the parent nucleoside, prodrug optimization and selection, and synthesis optimization of the development candidate **4b**. Candidate compound **4b** is currently in phase 2 trials to assess the effect on the chronic shedding of virus in EVD survivors following promising efficacy data established in a non-human primate EVD challenge model. These data have been recently reported¹⁷ and will be summarized along with the early clinical experience with **4b**.

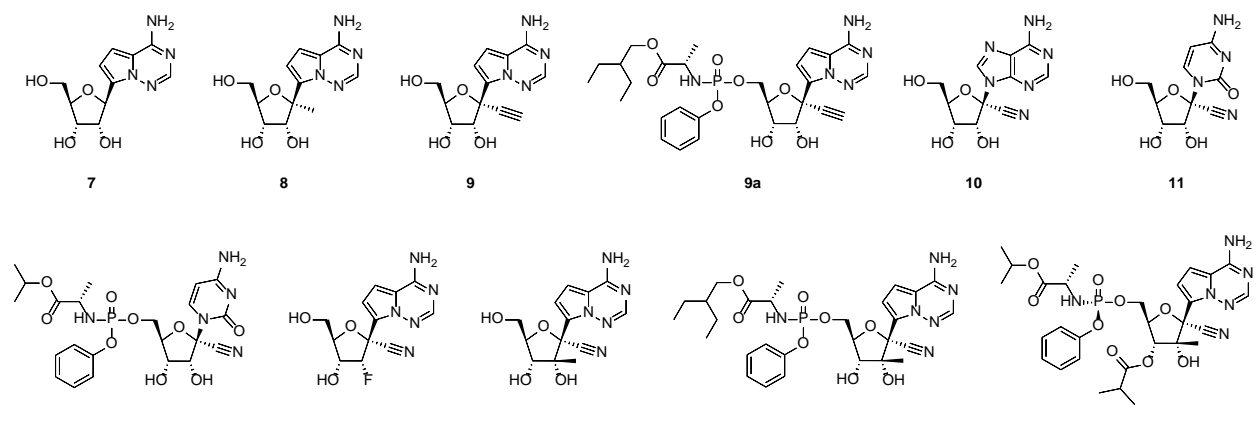
RESULTS AND DISCUSSION

The assembly of the ~1000 compound nucleos(t)ide screening library was heavily focused toward ribose analogs that could target RNA viruses since this would encompass many emerging viral infections ranging from respiratory pathogens belonging to the *coronaviridae* family such as severe acute respiratory syndrome (SARS) / Middle East respiratory syndrome (MERS), to mosquito-borne viruses of the *flaviviridae* family such as Dengue and Zika. Second, the library also contained selected monophosphate and nucleoside phosphonate prodrugs to capture analogs that may be missed in cellular screens due to either poor permeability or inefficient metabolism in the respective cell types that the different antiviral assays utilize. Nucleoside analogs require activation by intracellular nucleoside/tide kinases to generate their respective triphosphate (TP) metabolites in order to then compete with endogenous natural nucleotide pools for incorporation into the replicating viral RNA.¹⁷ The first phosphorylation step to generate the nucleoside monophosphate, is often rate limiting so the application of monophosphate prodrugs, especially phosphoramidates (ProTidesTM) has been extensively explored in nucleoside analogs to bypass this initial phosphorylation step.¹⁸ A notable example includes the phosphoramidate prodrug Sofosbuvir (**5**) for the treatment of HCV.¹⁹ Nucleoside phosphonate analogs are bioisosteres of the monophosphates but also require prodrugs to enable masking of the charged phosphonate acid thereby allowing more efficient entry into cells. A recent example of an approved drug in this class is the phosphonamidate prodrug tenofovir alafenamide (**6**) for the treatment of HIV.²⁰ In both examples the amidate prodrugs effectively deliver high levels of triphosphate (diphosphophosphonate in the case of nucleoside phosphonates) inside the target cells and demonstrate significant improvements in potency compared to their respective parent nucleos(t)ides when screened in antiviral assays (Figure 1).^{20,21}

In the original library screening toward a panel of RNA viruses across different viral families promising leads were identified. Subsequent to the EVD outbreak, some of these analogs were selected for EBOV testing in collaboration with the CDC and USAMRIID in a BSL-4 facility. From this screen nucleoside **4**²², a 1'-CN modified adenosine C-nucleoside discovered for HCV emerged with submicromolar activity towards EBOV in Human Lung Microvascular Endothelial Cells HMVEC cells (entry 2, Table 1). In addition, its phosphoramidate prodrug mixture **4a**²³

containing ~1:1 ratio of *Sp* (**4b**) (entry 3, Table 1) and *Rp* diastereoisomers was found to be very potent toward EBOV in both Hela and HMVEC cells. Encouraged by these data, the anti-EBOV activity for a range of nucleoside analogs and their prodrugs was evaluated and the results are reported in Table 1, along with activity toward respiratory syncytial virus (RSV), from the *pneumoviridae* family, and HCV, from the *flaviviridae* family.

Table 1. Structure Activity Relationships (SAR) of nucleoside parents and selected prodrugs.

								
Entry	Compound	EBOV EC ₅₀ Hela cells (μM)	EBOV EC ₅₀ HMVEC cells ³ (μM)	RSV EC ₅₀ HEp-2 cells (μM)	HCV 1b EC ₅₀ Huh-7 cells (μM)	CC ₅₀ HEp-2 cells (μM)	CC ₅₀ Huh-7 cells (μM)	CC ₅₀ MT4 cells (μM)
1	7	--	--	--	0.0035	0.038 ²	0.15	<0.01
2	4	>20	0.78	0.53	4.1	>100	>88	>57
3	4a	0.17	0.12	0.027	0.023 ²	9.2	17 ²	2.0
4	8	--	>10	5.5	38	93	62	4.5
5	9	--	--	>200	>88	>200	>88	120
6	9a	--	3.9	1.1	6.9	>100	>44	>32
7	10	--	56	>100	>44	>100	>88	>53
8	11	>50	>10	7.3	12	>100	>44	>57
9	11a	>20	--	63	2.5	>100	>44	53
10	12	--	--	>100 ¹	>44	--	>44	32 ²
11	13	50	>10	>100	>44	>100	>44	>57
12	13a	27	13 ²	>50	0.37	>50	>44	1.4
13	13b	>20	40	>20	0.31	95	51	7.8

¹96 well assay format. ²n=1 data only. ³HMVEC cells were TERT-immortalized human foreskin microvascular endothelial cells (ATCC-4025).

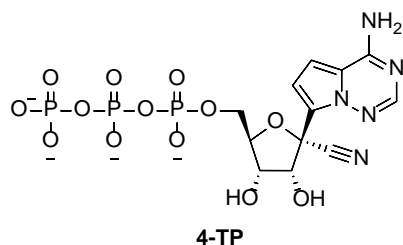
The presence of the 1'-CN modification in **4** was found to be critical in providing selectivity toward viral polymerases and avoiding the significant toxicity (CC₅₀<0.01 – 0.15 μM) associated with the unmodified *C*-nucleoside **7** (entry 1).²⁴ The MT4 cell line was also used, as a sensitive

cell line to evaluate cytostatic effects of nucleoside analogs, and confirmed the poor selectivity of **7** observed in both the HEP-2 and Huh-7 cell lines. The prodrug mixture **4a** in addition to potent anti-EBOV activity, demonstrated significant activity toward RSV and HCV, with potencies similar or better than that for EBOV ($EC_{50} < 120$ nM). The broad and potent antiviral activity across all three viruses for **4a** was further supported by the potent activity of the single Sp isomer **4b** toward other emerging RNA viruses such as MERS and Junin viruses, and to a lesser extent Lassa.¹⁷ The 1'-methyl analog **8** (entry 4) was less active toward EBOV and also displayed a higher degree of toxicity compared to the 1'-CN analog, illustrating how small changes in the polarity and size of the 1' substituent can impact the overall profile. The 1'-ethynyl analog **9** (entry 5)²² and its corresponding 2-ethylbutyl alanine prodrug **9a** (entry 6) were both less active when compared to their respective 1'-CN counterparts. Compound **4** is a C-nucleoside analog which provides chemical and enzymatic stability toward deglycosylation reactions at the anomeric center. However, alternate base modifications including *N*-nucleosides were also studied. Interestingly, the corresponding 1'-CN modified adenosine *N*-analog **10** (entry 7)²⁵ was significantly less active toward all viruses, whilst the 1'-CN modified *N*-nucleoside pyrimidine **11** (entry 8) retained some antiviral activity.^{26, 27} The phosphoramidate prodrug of 1'-CN cytidine **11a** (entry 9) did not improve the potency toward EBOV (in HeLa cell assay) presumably due to limitations in metabolism beyond the monophosphate. In general, the potency trends of 1' substitution and nucleobase changes were similar across EBOV, RSV and HCV which was in contrast to the trends uncovered with 2' modifications. The 2'-deoxy-2'-fluorine analog **12** (entry 10) and the 2'-β-methyl analog **13** (entry 11) both lacked significant antiviral activity. However, the 2'-β-methyl phosphoramidate prodrugs, analogs **13a** and **13b** (entries 12 and 13) respectively, were both potent toward HCV, and only weakly active/inactive toward EBOV and RSV. This result suggests that HCV polymerase is more able to accommodate the 2'-β-methyl group compared to the EBOV and RSV polymerases. Taken together with the 1' substitution and nucleobase SAR, the EBOV and RSV polymerases demonstrated similar activity trends, whilst HCV polymerase was differentiated in SAR at the 2' position.

To interrogate the cell based SAR more rigorously the active nucleoside triphosphate (NTP) metabolite e.g. **4-TP**²³ was tested toward the viral polymerases. The triphosphate **4-TP**

demonstrated a half-maximal inhibitory concentration of 1.1 μM against the RSV RdRp and 5.0 μM against HCV RdRp (Table 2). The Ebola viral polymerase has to date evaded efforts toward its isolation and expression so the intrinsic activity of the active NTP metabolite cannot be directly evaluated. An alternate method for estimating the inhibitory properties of an NTP for its viral target is to measure the NTP levels inside cells following incubation with the parent or prodrug compound at a given concentration, and then calculate the NTP levels at the EC_{50} measured in the same cells. In a continuous 72-h incubation of 1 μM **4b** the **4-TP** concentrations reached a C_{max} of 300, 110, and 90 μM in macrophages, HMVEC, and Hela cells lines respectively. When correlated to the EVD EC_{50} s in these respective cell types (Table 1) a half-maximal inhibitory concentration of approximately 5 μM was calculated for the intracellular inhibition of EBOV polymerase. This is several-fold weaker than the potency toward RSV polymerase, but similar to HCV polymerase supporting the comparable antiviral EC_{50} data demonstrated for the prodrug mixture **4a** across the three viruses when allowing for cell type differences (Table 1). The selective inhibition of the viral polymerases versus host polymerases is considered a key factor in the development of a safe and effective nucleoside antiviral.^{28, 29} Therefore the **4-TP** was evaluated toward several host polymerases and was found to be a weak incorporator toward mtRNA Pol, and not a substrate for DNA pol γ , as would be expected given the presence of the ribose 2' OH (Table 2). Across the host RNA and DNA polymerases evaluated there was no inhibition up to 200 μM (Table 2) demonstrating a high degree of selectivity of **4-TP** toward the viral polymerases.

Table 2. Inhibition of the RSV and HCV RdRps and human host polymerases by 4-TP.



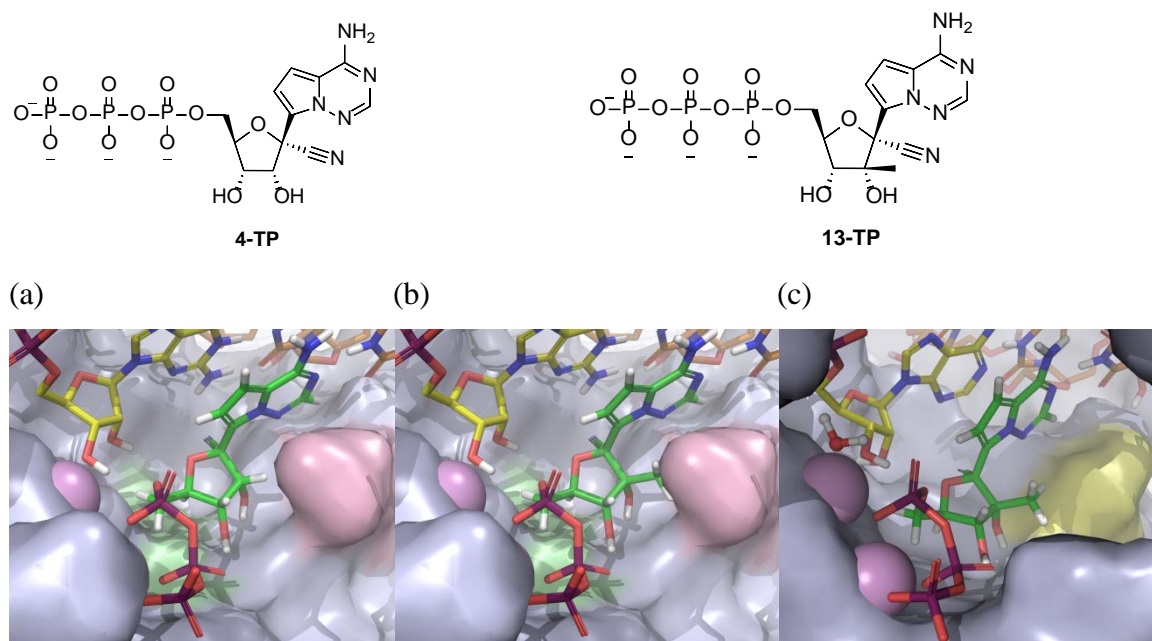
Enzyme	NTP IC_{50} (μM)	NTP SNI ¹ rate (%)
RSV RdRp	1.1	-
HCV RdRp	5	-
mtRNA Pol	>200	6

RNA Pol II	>200	-
DNA Pol α	>200	-
DNA Pol β	>200	-
DNA Pol γ	>200	0

¹SNI = Single Nucleotide Incorporation

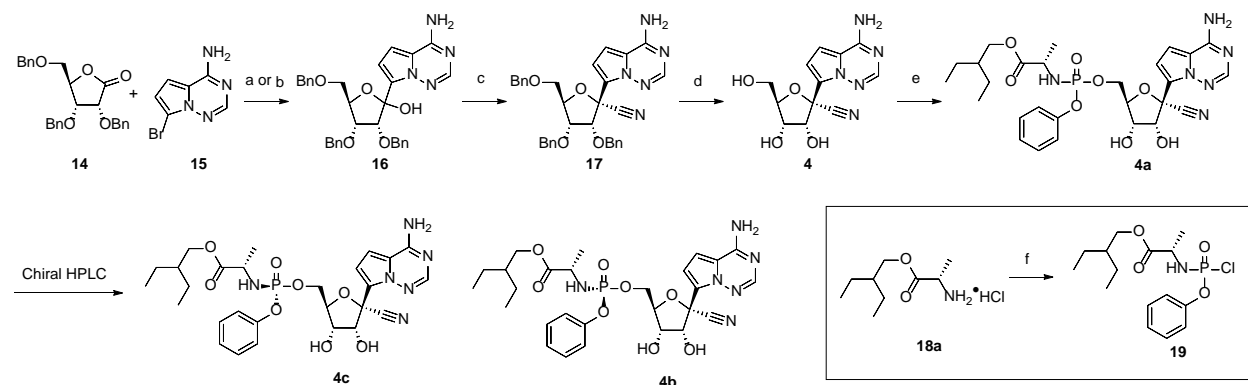
Molecular structure information is not available for the EBOV or RSV polymerases so modeling of the active sites was performed based on the published structures for HIV and HCV polymerases, together with an analysis of the respective sequences.³⁰ Within the modeled active site of EBOV polymerase the major difference between EBOV and RSV is Y636 (EBOV) compared to F704 (RSV) and the major difference between EBOV and HCV is E709 (EBOV) compared to S282 (HCV).³¹ On docking the triphosphate **4-TP**, the 1'-CN group occupies a pocket formed by residues that are identical between EBOV and RSV, yet very different in HCV (Figure 2a). Nevertheless the 1'-CN analog retains potency across these viruses. Moreover, the 1'-CN analog should retain its potency across a wide range of filovirus polymerases that could emerge in the future. The 2'- β -H of **4-TP** is in close proximity to E709 and replacement of this group with a 2'- β -methyl (compound **13** triphosphate) would be anticipated to interfere with E709 (Figure 2b). However, the 2'- β -methyl can be accommodated by the larger pocket afforded by the smaller S282 residue of HCV (Figure 2c). This suggests the lack of activity for 2'- β -methyl analogs toward EBOV and RSV and retained potency toward HCV is likely due to steric constraints in the polymerase active site. Consistent with the model, EBOV and RSV both have the E709 or equivalent residue, and compound 13 triphosphate was found to be significantly less active ($IC_{50} > 30 \mu M$) toward RSV (data not shown).

Figure 2. (a) Compound **4-TP** (green stick) modeled into EBOV polymerase active site. Residue Y636 is highlighted in green surface, sits below the ribose, and corresponds to F704 in RSV. Residue E709 is highlighted in red surface, sits in proximity to the 2'- β -H position of the ribose, and corresponds to S282 in HCV; (b) compound **13-TP** (green stick) modeled into the EBOV polymerase active site. The 2'- β -methyl overlaps with residue E709 highlighted in red. (c) Compound **13-TP** modeled into the HCV polymerase active site. Residue S282 is highlighted in the yellow surface and the 2'- β -methyl can be accommodated.



The screening and modeling efforts established **4** as the best lead for prodrug optimization. The ability to evaluate prodrugs, especially in vivo, required an efficient synthesis route for both the parent **4** and preferably single prodrug diastereoisomers. Neither was available at the outset so significant chemistry resources were applied to improve the robustness and scalability of the route along with generation of single diastereoisomers. The first generation synthesis of **4** and the single *Sp* phosphoramidate prodrug **4b** commenced with a glycosylation reaction via metal-halogen exchange of the bromo-base **15** followed by addition into the ribolactone **14** (Scheme 1). Two conditions were identified to render this desired C-C bond formation. The first condition (a) proceeded through addition of excess *n*-BuLi to a mixture of TMSCl and **15**, which was designed to result in lithium-halogen exchange after removal of the acidic 6N protons by silyl protection. Addition of this in situ generated reagent to the ribolactone **14** then afforded **16** in 25% yield.^{23,33,34} The alternative conditions (b) employed sodium hydride and 1,2-bis(chlorodimethylsilyl)ethane for the 6N protection step, followed by lithium-halogen exchange, and addition to the lactone to afford **16** in 60% yield.^{22,35}

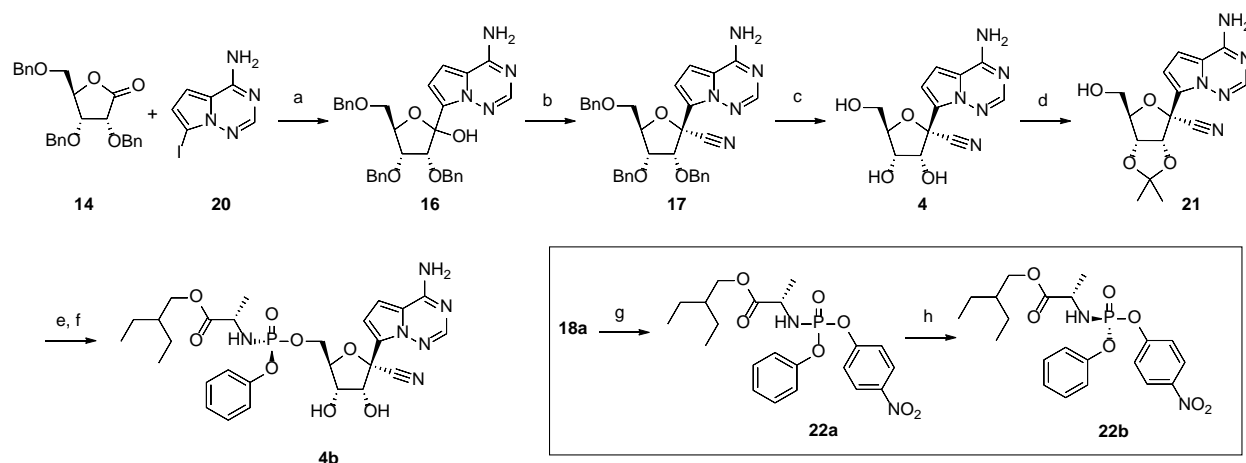
Scheme 1. First generation synthesis of 4a.^a



^aReagents and conditions: (a) *n*-BuLi, TMSCl, THF, -78°C , 25%; (b) 1,2-bis(chlorodimethylsilyl)ethane, NaH, *n*-BuLi, THF, -78°C , 60%; (c) TMSCN, $\text{BF}_3 \cdot \text{Et}_2\text{O}$, CH_2Cl_2 , -78°C , 58% (89:11 β -**17**/ α). (d) BCl_3 , CH_2Cl_2 , -78°C , 74%. (e) **19**, NMI, $\text{OP}(\text{OMe})_3$, 21%; (f) $\text{OP}(\text{OPh})\text{Cl}_2$, Et_3N , CH_2Cl_2 , 0°C , 23%.

The efficiency of both conditions was suboptimal as the yields were capricious and highly dependent on the cryogenic temperatures and the rate of *n*-BuLi addition required for the transformation. Furthermore, premature quenching and reduction of lithio base was observed, which was rationalized to be a consequence of deprotonation α to the lactone under the highly basic conditions. Compound **16** was isolated as a mixture of 1'-isomers which were taken into the subsequent 1'-cyanation reaction to isolate the major product, β -anomer **17**, by chromatography.³⁵ Following removal of the three benzyl protecting groups to afford **4**, the diastereomeric mixture of the phosphoramidoyl chloridate prodrug moiety **19**, was then coupled to provide **4a** in 21% yield, as an ~1:1 diastereomeric mixture.²³ The two diastereomers were resolved using chiral HPLC to afford the *Sp* isomer **4b** and *Rp* isomer **4c** respectively.³⁶ While this route initially provided quantities of **4b** the variability in yields, suboptimal selectivity, frequent use of cryogenic temperatures, and chiral chromatography, hindered this route from being suited to larger scales.

Scheme 2. Second generation synthesis of 4b.^a



^aReagents and conditions: (a) TMSCl, PhMgCl, *i*-PrMgCl•LiCl, THF, -20 °C, 40%; (b) TMSCN, TfOH, TMSOTf, CH₂Cl₂, -78 °C, 85%; (c) BCl₃, CH₂Cl₂, -20 °C, 86%; (d) 2,2-dimethoxypropane, H₂SO₄, acetone, rt, 90%; (e) MgCl₂, (*i*-Pr)₂NEt, MeCN, 50 °C, 70%; (f) 37% HCl, THF, rt, 69%. (g) OP(OPh)Cl₂, Et₃N, CH₂Cl₂, -78 °C, then 4-nitrophenol, Et₃N, 0 °C, 80%; (h) *i*-Pr₂O, 39%.

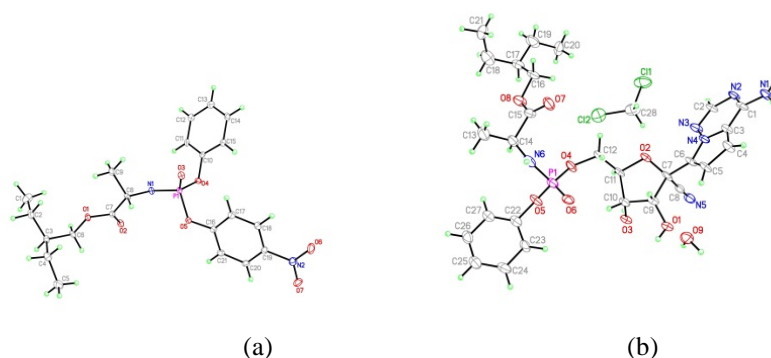
The second generation route enabled the diastereoselective synthesis of the single *Sp* isomer **4b** on scales suitable to advance the compound into preclinical efficacy and toxicity studies (Scheme 2).¹⁷ The glycosylation step employed the iodo-base **20** instead of the bromo base which enabled a more facile metal-halogen exchange compatible with *i*-PrMgCl•LiCl complex.³⁷ Treatment with PhMgCl and TMSCl provided 6N protection to remove the acidic protons with a higher degree of control, and addition of *i*-PrMgCl•LiCl followed by the ribolactone **14** at -20 °C afforded the glycosylation product **16** in a 40% yield. The milder reagents and temperature enabled large-scale batches to be carried out with consistent yields. Treatment of **16** with TMSCN, TMSOTf, and TfOH at -78 °C afforded **17** in 85% yield in >95:5 anomeric ratio. The inclusion of TfOH was key to promote the high yield and high selectivity favoring the desired β-anomer. Benzyl deprotection was effected through treatment with BCl₃ and **4** was readily isolated through crystallization. Acetonide protection of the 2',3'-hydroxyl moieties with 2,2-dimethoxypropane in the presence of H₂SO₄ afforded **21** in 90% yield. Utilizing the 2',3'-acetonide protection was found to be optimal as the yield of the coupling reaction with the *p*-nitrophenolate 2-ethylbutyl-L-alaninate prodrug mixture **22a** was dramatically improved compared to directly coupling to the unprotected nucleoside **4** (70% vs 40%). In the event, reaction of **21** with the single *Sp* isomer of the *p*-nitrophenolate prodrug precursor **22b** in the presence of MgCl₂ and Hunig's base efficiently appended the prodrug group

in 70% yield as a single *Sp* isomer. Final deprotection of the acetonide with concentrated HCl in THF afforded **4b** in 69% yield.

The single *Sp* isomer **22b** of the *p*-nitrophenolate 2-ethylbutyl-L-alaninate prodrug precursor **22a** was prepared through a sequence beginning with exposure of 2-ethylbutyl-L-alanine **18** with OP(OPh)Cl₂ followed by 4-nitrophenol to the diastereomeric mixture at phosphorus, **22a**. Importantly, the single *Sp* isomer **22b** was readily resolved from the mixture in 39% yield through crystallization in diisopropyl ether, a discovery that was paramount for the success of the diastereoselective synthesis of the **4b**.³⁸ Thus, utilizing the *p*-nitrophenolate 2-ethylbutyl-L-alaninate prodrug coupling partner **22b** offered a significant advantage over the chloridate **19** in the first generation sequence. Overall the second generation synthesis of **4b** offered the following improvements: (1) milder glycosylation conditions at higher temperature to allow for consistent yields and scalability, (2) higher selectivity and yield for the 1'-cyanation reaction, and (3) a highly efficient coupling sequence of a single *Sp* prodrug moiety for the diastereoselective synthesis of **4b**. Through this second generation route >200g was rapidly prepared to support preclinical efficacy and toxicity studies.

The stereochemistry of the *p*-nitrophenolate 2-ethylbutyl-L-alaninate prodrug **22b** and candidate compound **4b** were unambiguously assigned by small molecule X-Ray crystallography (Figure 3). In both cases the *Sp* isomer was established and suggests that the coupling with the nucleoside and reagent follows a S_N2 type inversion of the phosphorus stereocenter.

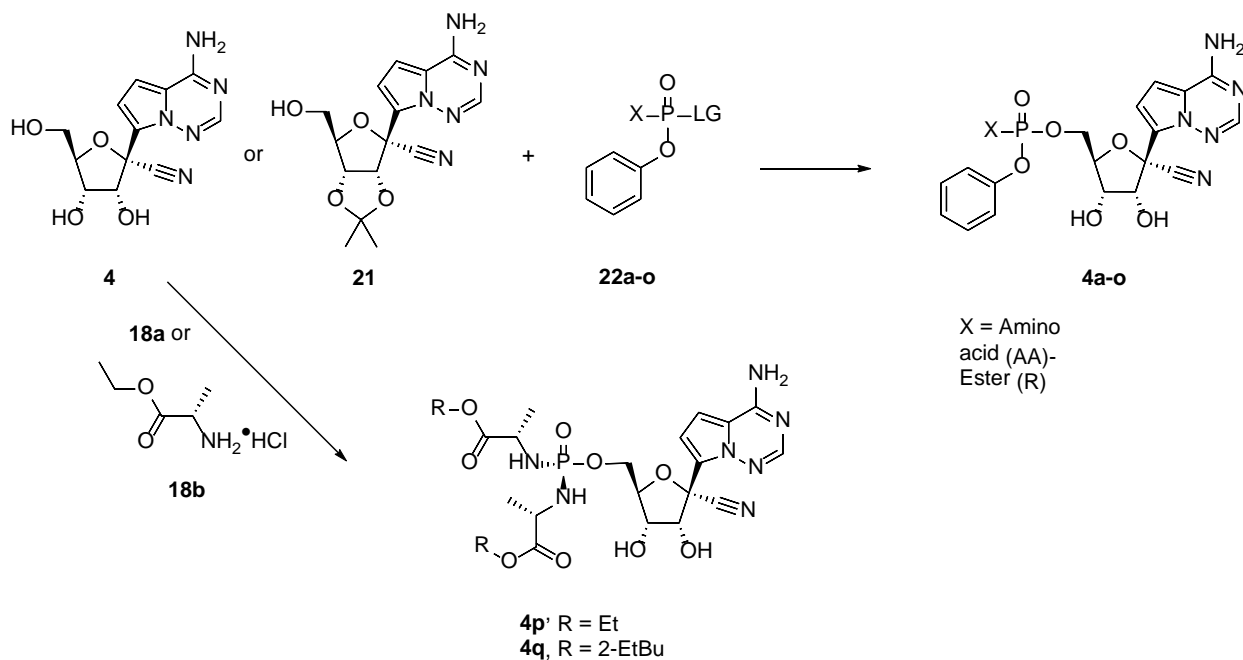
Figure 3. Thermal ellipsoid representations of (a) **22b** and (b) **4b**.



The improved method for preparing **4** enabled many monophosphoramidate (ProTideTM) and bisphosphoramidate prodrug analogues to be synthesized, the results of which are summarized in

Scheme 3. A number of conditions were identified to affect the coupling of the prodrug moieties to **4** or the 2',3'-acetonide protected analogue **21**. The reactions employing **4** proceeded under either Brønsted basic conditions utilizing *t*-BuMgCl or Lewis acidic conditions with MgCl₂ in polar aprotic solvents to afford the desired prodrugs **4d-n** in yields ranging from 24-43%. The coupling reaction of the 2',3'-acetonide protected analogue **21** under lewis acidic conditions followed by in-situ acetonide deprotection in general afforded much higher yields ranging from 60-70% (analogue **4b** and **4o**). Both the *para*-nitrophenol (PNP) and penta-fluorophenol (PFP) prodrug electrophiles were compatible in the coupling reactions and achieved comparable yields. The reactions utilizing a ~1:1 diastereomeric mixture of the prodrug electrophiles, **22a**, **d-i**, **k-m** provided the prodrug products in 1.5-2.6 to 1 diastereomeric ratios at phosphorus. In addition to the monophosphoramidate prodrugs, two bisphosphoramidate prodrugs **4p** and **4q** were synthesized and evaluated since they avoided the preparation of chiral phosphorus reagents.

Scheme 3. Prodrug Synthesis.



Prodrug ¹	X		LG ³	Coupling Partner	Conditions	Product	Yield	Isomer Ratio
	Ester R	AA ²						
22a	2-EtBu	L-Ala	PNP	4	<i>t</i> -BuMgCl, THF, DMF, rt	4a	43%	2.5 : 1
22b⁴	2-EtBu	L-Ala	PNP	21	MgCl ₂ , (<i>i</i> -Pr) ₂ NEt, THF, 50 °C; conc. HCl, 0 °C	4b	69%	Sp Isomer
22d	Et	L-Phe	PNP	4	<i>t</i> -BuMgCl, THF, DMF, rt	4d	34%	2.6 : 1

22e	Et	L-Val	PNP	4	<i>t</i> -BuMgCl, THF, NMP, rt	4e	43%	1.8 : 1
22f	Et	AIB	PNP	4	<i>t</i> -BuMgCl, THF, NMP, 50 °C	4f	25%	1.5 : 1
22g	Et	L-Ala	PNP	4	<i>t</i> -BuMgCl, THF, NMP, rt	4g	24%	2.5 : 1
22h	CH ₂ c-Pr	L-Ala	PNP	4	MgCl ₂ , (<i>i</i> -Pr) ₂ NEt, DMF, 50 °C	4h	38%	1.9 : 1
22i	<i>c</i> -Bu	L-Ala	PNP	4	MgCl ₂ , (<i>i</i> -Pr) ₂ NEt, DMF, 50 °C	4i	37%	3 : 2
22j ⁴	<i>i</i> -Pr	L-Ala	PNP	4	<i>t</i> -BuMgCl, THF, NMP, 50 °C	4j	38%	Sp Isomer
22k	<i>t</i> -Bu	L-Ala	PNP	4	MgCl ₂ , (<i>i</i> -Pr) ₂ NEt, DMF, 50 °C	4k	32%	1.5 : 1
22l	CH ₂ c-Bu	L-Ala	PNP	4	<i>t</i> -BuMgCl, THF, DMF, rt	4l	36%	1.7 : 1
22m	3-Pent	L-Ala	PNP	4	MgCl ₂ , (<i>i</i> -Pr) ₂ NEt, DMF, 50 °C	4m	42%	1.5 : 1
22n ⁵	<i>c</i> -Pent	L-Ala	PFP	4	<i>t</i> -BuMgCl, THF, DMF, rt	4n	43%	27 : 1
22o	2-EtBu	D-Ala	PNP	21	MgCl ₂ , (<i>i</i> -Pr) ₂ NEt, THF, 50 °C; conc. HCl, 0 °C	4o	66%	1.1 : 1
18b	Et	L-Ala	NA	4	POCl ₃ , PO(OMe) ₃ , Et ₃ N, rt	4p	16%	NA
18a	2-EtBu	L-Ala	NA	4	POCl ₃ , PO(OMe) ₃ , Et ₃ N, rt	4q	58%	NA

¹ Prodrug is an undetermined mixture of diastereoisomers unless otherwise indicated, ² AA = amino acid, ³ LG = Leaving Group, ⁴ Single Sp isomers, ⁵ Reagent was predominantly a single unassigned isomer at phosphorus, Ala = Alanine, Phe = Phenylalanine, AIB = 2-aminoisobutyrate, Et = ethyl, cPr = cyclopropyl, cBu = cyclobutyl, cPent = cyclopentyl, Pent = pentyl, iPr = isopropyl, tBu = *tert* butyl, 2-EtBu = 2-ethylbutyl, PNP = *para*-nitrophenolate, PFP = pentafluorophenolate, rt = room temperature.

The monophosphate prodrugs can improve the potency of the parent nucleosides substantially by delivering the monophosphate into cells and effectively bypassing a rate limiting first phosphorylation step. The phenol and amino acid esters mask the negative charge of the monophosphate group enabling facile passive penetration into the cell. The prodrug breakdown is initiated by intracellular esterases (e.g. carboxy esterase 1, cathepsin A) that cleave the ester unraveling the carboxylate moiety, which then continues to breakdown to the monophosphate that serves as the precursor to synthesis of the intracellular NTP.¹⁷

Prodrugs **4a-q** were evaluated toward EBOV in three cell lines and for stability properties in human plasma (Table 3). In general the antiviral activity trends for EBOV across all three cell lines were similar supporting the efficient conversion of these prodrugs across multiple different cell types. A series of ethyl esters with differing amino acids (entries 2-5), established the phenylalanine and alanine amino acids were the most promising but the potency improvements were modest compared to parent **4** (Table 1). Evaluation of different esters of alanine with increasing lipophilicity (log D) ranging from 0.6 to 2.1 (entries 5-13) demonstrated increased potency as lipophilicity increased, unless the ester contained proximal branching e.g. iPr entry 8, tBu entry 9, or 3-pentyl entry 11. In these proximally branched examples the increased steric hindrance is presumed to slow down the cleavage rate by esterases. Cyclic esters e.g. cBu (entry 7) and cPent (entry 12) are however more potent despite the proximal branching. Given the

intended route of administration was intravenous, increasing lipophilicity beyond log D~2 was not explored due to solubility concerns. The D-Ala 2-EtBu mixture (entry 16) was less potent than the corresponding L-Ala analog (entry 13) and the two bisphosphoramidate prodrugs (entries 17 and 18) also had reduced activity compared to their monoamidate counterparts (entries 5 and 13 respectively). Thus, based on antiviral properties across HeLa and HMVEC cells, the most promising initial monophosphoramidate prodrug mixtures were the CH₂cBu **4l** and 2-EtBu **4a** esters (entries 10 and 13). The *Sp* and *Rp* isomers of **4a** (entries 14 and 15 respectively) were separated and found to be similar in potency. For the intended i.v. route of administration, plasma stability was not deemed critical in the selection process provided sufficient stability ($t_{1/2}$ > 60 min) was maintained to allow loading of target cells harboring the virus during drug infusion. A key driver for the selection of **4b** as oppose to **4c** or the **4l** isomers was the crystalline nature of the *Sp* prodrug reagent **22b** that allowed rapid scale up for efficacy and IND enabling studies of the single *Sp* isomer **4b**.

Table 3. Antiviral activity of prodrugs 4a-q.

Entry	Compound	Ester	AA ¹	EBOV EC ₅₀ HeLa (nM)	EBOV EC ₅₀ HMVEC ² (nM)	EBOV EC ₅₀ Macro ³ (nM)	CC ₅₀ MT4 (μM)	Human Plasma $t_{1/2}$ (min)	LogD
1	4	-	-	>20000	780	>20000	>57	-	0.3
2	4d	Et	L-Phe	4380	587	270	15	1584	1.6
3	4e	Et	L-Val	7040	3151	-	>100	1584	1.2
4	4f	Et	AIB	8470	1585	-	>100	1584	0.9
5	4g	Et	L-Ala	2425	636	-	13	1584	0.6
6	4h	CH ₂ cPr	L-Ala	570	306	-	5	249	1.0
7	4i	cBu	L-Ala	420	88	-	6	815	1.1
8	4j	iPr	L-Ala	1845	367	297	21	1561	1.1
9	4k	tBu	L-Ala	30410	3790	-	>100	1584	1.3
12	4n	c-Pent	L-Ala	633	160	120	8.8	1578	1.3
10	4l	CH ₂ cBu	L-Ala	160	72	-	3	220	1.5
11	4m	3-Pent	L-Ala	1810	845	-	>100	860	1.6
13	4a	2-EtBu	L-Ala	170	121	100	2	195	2.1
14	4c	2-EtBu	L-Ala	80	53	111	3	234	2.0
15	4b	2-EtBu	L-Ala	100	53	86	2	69	2.1
16	4o	2-EtBu	D-Ala	550	518	729	42	1584	2.1
17	4p	Et	L-Ala	20420	9102	-	>53		<0.3
18	4q	2-EtBu	L-Ala	970	678	-	9	507	2.7

¹ AA = Amino Acid, ²HMVEC = TERT-immortalized human foreskin microvascular endothelial cells (ATCC-4025), ³Macro = human macrophages. Ala = Alanine, Phe = Phenylalanine, AIB = 2-aminoisobutyrate, Et = ethyl, cPr = cyclopropyl, cBu = cyclobutyl, cPent = cyclopentyl, Pent = pentyl, iPr = isopropyl, tBu = *tert* butyl, 2-EtBu = 2-ethylbutyl

In vivo efficacy evaluation of **4b** was conducted in monkeys since this represented the most relevant animal model of EVD with similar pathophysiology to the actual human disease. In addition, phosphoramidate esters are highly prone to plasma metabolism in rodents on account of high expression of plasma carboxylesterases³⁹ thereby excluding pilot efficacy studies in small animal models. Due to the high first pass hepatic extraction of phosphoramidates, oral administration was also not explored in favor of injectable routes of administration. Moreover, oral delivery in patients acutely infected with EBOV that are demonstrating symptoms of the disease may not be ideal because gastrointestinal symptoms may limit the dose that is effectively absorbed. Intravenous administration of **4b** in rhesus monkeys demonstrated rapid elimination of prodrug and appearance of parent nucleoside in systemic circulation. However **4b** also rapidly distributed to peripheral blood mononuclear cells (PBMCs) and triphosphate levels in PBMCs were elevated to a maximum within 2h. A dose of 10 mg/kg resulted in an estimated PBMC triphosphate level at 24 h that was several fold higher than the estimated IC₅₀ of 5 µM for EBOV, with a half-life of 14h similar to that measured in vitro in human macrophages. The long intracellular half-life of **4-TP** supported once daily i.v. administration in the rhesus efficacy study and in the clinical development program.

Establishment of preclinical in vivo efficacy for **4b** was conducted in a EBOV-infected rhesus challenge model with dose levels up to 10 mg/kg i.v., initiated at different times post infection. These studies have recently been published in full and will only be summarized.¹⁷ In the first part of the study, **4b** was dosed i.v. at 3 mg/kg on day 0 or day 2 relative to EBOV inoculation, and continued once daily for 12 days. Systemic viremia was reduced and survival out to day 28 post infection was improved. Animals administered 3 mg/kg **4b** starting at day 0, had a survival rate of 33% whilst those initiated on day 3 had a 66% survival at 28 days. This encouraging data was then followed with a second study in which one arm explored dosing initiation on day 3 with 10 mg/kg daily for 12 days, and two other arms explored an initial loading dose of 10 mg/kg on day 2 or day 3, followed by eleven 3 mg/kg daily maintenance doses. All the animals in the two arms beginning on day 3 (n=12 total) survived through day 28, the end of study. In the daily 10 mg/kg dosed group the effect on viremia was consistently

greater than in any of the other groups and was below the limit of detection (8×10^4 RNA copies ml⁻¹) in 4 of the 6 animals on days 5 and 7 relative to the vehicle-treated control where the geometric mean exceeded 10^9 copies ml⁻¹ at these time points. This data established the effectiveness of **4b** in treatment of EVD in NHPs and accelerated its progress into clinical development. In addition to the efficacy studies, distribution studies in cynomolgus monkeys using [¹⁴C]GS-5734 at the same effective dose of 10 mg/kg established the presence of drug related products in the potential sanctuary sites for the virus including testes, epididymis, eyes and brain. These data supported the potential that **4b** treatment may also reduce virus replication in these sanctuary sites.

Safety and pharmacokinetics of **4b** administered as once-daily i.v. infusion were evaluated in single and multiple dose phase 1 clinical trials. No serious adverse effects of the drug were observed. During the course of the phase 1 studies two requests for a compassionate use of **4b** were received. The first case involved a healthcare worker who had survived acute infection but had relapsed with symptoms of acute meningoencephalitis.⁴⁰ Ebola virus was detected both systemically in plasma and in cerebrospinal fluid. When treated with monoclonal antibodies, the patient developed adverse reaction and was subsequently treated with supportive therapy and **4b** for a period of 14 days beginning with a dose of 150 mg and then increasing to 225 mg after 2 daily infusions. No serious adverse effects related to drug were observed. The patient recovered and cleared the virus from both plasma and CNS although without proper control or natural history data to compare, it is not clear whether the antiviral therapy was effective. The second case involved newborn infant congenitally infected with EBOV and treated with ZMapp, blood transfusion and subsequently **4b**.⁴¹ The infant recovered and was eventually declared free of Ebola virus after repeated testing failed to detect viremia. The unprecedented scale of the West African epidemic and the ability to reduce mortality rates through supportive therapy has resulted in many Ebola survivors of Ebola virus disease. The persistence of virus sequelae in survivors in multiple body compartments has now been documented in addition to secondary sexual transmission via virus in genital secretions.⁴ This has prompted the initiation of randomized, blinded, placebo-controlled phase 2 study (PREVAIL IV) which plans to enroll at least 60 adult male survivors to receive either 100 mg **4b** or placebo once-daily over 5 days to assess the effect of **4b** therapy on the viral shedding in semen.⁴² The

results of this study could provide the first evidence as to the potential of **4b** to reduce virus replication in humans.

SUMMARY

The recent Ebola outbreak prompted the urgent need for antiviral therapeutics for the treatment of Ebola. We identified a promising nucleotide therapeutic **4b** through initial screening and subsequent optimization of the prodrug moiety for i.v. administration. The partnership with government organizations, including CDC and USAMRIID, that generated the screening data and conducted the rhesus efficacy studies was critical to the successful identification of **4b**. Also of importance was the significant chemistry effort that rapidly identified a more efficient route to the parent compound **4** and the ability to prepare, through crystallization of a key reagent, the single *Sp* phosphorus diastereoisomer **4b** for in vivo model studies. The active triphosphate delivered by the prodrug has low micromolar polymerase activity toward EBOV, high selectivity for the viral polymerase compared to host polymerases, and a long intracellular half-life supporting QD administration. Parenteral treatment with **4b** in Ebola infected NHPs at 10 mg/kg over 12 days demonstrated a substantial antiviral effect along with 100% survival. Based on its promising potential, and preliminary safety data from phase 1 studies, regulatory authorities approved the compassionate use of **4b** in two cases including an newborn infant with EVD. Further clinical data on **4b** is being collected in the phase 2 PREVAIL IV study that aims to assess the ability of **4b** to reduce Ebola virus replication in sanctuary sites of survivors.

Acknowledgements

We acknowledge the contributions of the following individuals at USAMRIID for scientific input, T Bocan, A Duplantier, R Panchal, C Kane, and for services performed, S Tritsch, C. Retterer, D. Gharaibeh, T. Kenny, B. Eaton, G Gomba, and C Rice. From Gilead Sciences we acknowledge K. Wang, K. Brendza, T. Alfredson and L. Serafini who assisted with analytical methods, S. Bondy and R. Seemayer procured key raw materials, L. Heumann, R. Polniaszeck, E. Rueden, A. ChtChemelinine, K. Brak and B. Hoang contributed to synthesis, and Yelena Zherebina to chiral separations. These studies were in part supported by The Joint Science and Technology Office for Chemical and Biological Defense (JSTO-CBD) of the Defense Threat Reduction Agency (DTRA) under plan #CB10218.

Experimental Section

All organic compounds were synthesized at Gilead Sciences, Inc (Foster City, CA) unless otherwise noted. Commercially available solvents and reagents were used as received without further purification. Nuclear magnetic resonance (NMR) spectra were recorded on a Varian Mercury Plus 400 MHz at room temperature, with tetramethylsilane as an internal standard. Proton nuclear magnetic resonance spectra are reported in parts per million (ppm) on the δ scale and are referenced from the residual protium in the NMR solvent (chloroform- d_1 : δ 7.26, methanol- d_4 : δ 3.31, DMSO- d_6 : δ 2.50). Data is reported as follows: chemical shift [multiplicity (s = singlet, d = doublet, t = triplet, q = quartet, p = pentet, sep = septet, m = multiplet, br = broad, app = apparent), coupling constants (J) in Hertz, integration. Carbon-13 nuclear magnetic resonance spectra are reported in parts per million on the δ scale and are referenced from the carbon resonances of the solvent (chloroform- d_1 : δ 77.16, methanol- d_4 : δ 49.15, DMSO- d_6 : δ 39.52). Data is reported as follows: chemical shift. No special nomenclature is used for equivalent carbons. Phosphorus-31 nuclear magnetic resonance spectra are reported in parts per million on the δ scale. Data is reported as follows: chemical shift [multiplicity (s = singlet, d = doublet, t = triplet), coupling constants (J) in Hertz. No special nomenclature is used for equivalent phosphorus resonances. Analytical thin-layer chromatography was performed using Merck KGaA Silica gel 60 F₂₅₄ glassplates with UV visualization. Preparative normal phase silica gel chromatography was carried out using a Teledyne ISCO CombiFlash Companion instrument with silica gel cartridges. Purities of the final compounds were determined by high-performance liquid chromatography (HPLC) and were greater than 95% unless otherwise noted. HPLC conditions to assess purity were as follows: Agilent 1100 Series HPLC, Phenomenex Kinetex C18, 2.6 μ m 100Å, 100 \times 4.6 mm column; 2-98% gradient of 0.1% trifluoroacetic acid in water and 0.1% trifluoroacetic acid in acetonitrile; flow rate, 1.5 mL/min; acquisition time, 8.5 min; wavelength, UV 214 and 254 nm. High-resolution mass spectrometry (HRMS) was performed on an Agilent model 6230 Accurate Mass Time of Flight Mass Spectrometer featuring Agilent Jet Stream Thermal Focusing Technology, with an Agilent 1200 Rapid Resolution HPLC. HRMS chromatography was performed using an Agilent Zorbax Eclipse Plus C18 RRHD 1.8 μ m, 2.1 \times 50 mm column at 30 °C, with a 10-90% gradient of 0.05% trifluoroacetic acid in water and 0.05% trifluoroacetic acid in acetonitrile. LC/MS was conducted on a Thermo

Finnigan MSQ Std using electrospray positive and negative $[M + 1]^+$ and $[M - 1]^-$, and a Dionex Summit HPLC System (model: P680A HPG) equipped with a Gemini 5 μ C18 110A column (30 mm \times 4.60 mm), eluting with 0.05% formic acid in 1% acetonitrile/water and 0.05% formic acid in 99% acetonitrile/water.

The synthesis, characterization data, and associated references for the following compounds are provided in supporting information: **4**, **4a**, **7-11**, **11a**, **12-13**, **13a**, **13b**, **4-TP**, **13-TP**, **18a-b**, **19**, **21**, and **22a-o**.

(S)-2-ethylbutyl 2-(((S)-(((2R,3S,4R,5R)-5-(4-aminopyrrolo[2,1-f][1,2,4]triazin-7-yl)-5-cyano-3,4-dihydroxytetrahydrofuran-2-yl)methoxy)(phenoxy)phosphoryl)amino)propanoate (4b).

Compound **4b** was prepared from **4** and **22b** as described previously.¹⁷

¹H-NMR (400 MHz, methanol-*d*₄): δ 7.86 (s, 1H), 7.33 – 7.26 (m, 2H), 7.21 – 7.12 (m, 3H), 6.91 (d, *J* = 4.6 Hz, 1H), 6.87 (d, *J* = 4.6 Hz, 1H), 4.79 (d, *J* = 5.4 Hz, 1H), 4.43 – 4.34 (m, 2H), 4.28 (ddd, *J* = 10.3, 5.9, 4.2 Hz, 1H), 4.17 (t, *J* = 5.6 Hz, 1H), 4.02 (dd, *J* = 10.9, 5.8 Hz, 1H), 3.96 – 3.85 (m, 2H), 1.49 – 1.41 (m, 1H), 1.35 – 1.27 (m, 8H), 0.85 (t, *J* = 7.4 Hz, 6H). ¹³C-NMR (100 MHz, methanol-*d*₄): δ 174.98, 174.92, 157.18, 152.14, 152.07, 148.27, 130.68, 126.04, 125.51, 121.33, 121.28, 117.90, 117.58, 112.29, 102.60, 84.31, 84.22, 81.26, 75.63, 71.63, 68.10, 67.17, 67.12, 51.46, 41.65, 24.19, 20.56, 20.50, 11.33, 11.28.; ³¹P-NMR (162 MHz, methanol-*d*₄): δ 3.66 (s); HRMS (*m/z*): $[M]^+$ calcd for C₂₇H₃₅N₆O₈P, 602.2254; found, 602.2274.

(S)-2-ethylbutyl 2-(((R)-(((2R,3S,4R,5R)-5-(4-aminopyrrolo[2,1-f][1,2,4]triazin-7-yl)-5-cyano-3,4-dihydroxytetrahydrofuran-2-yl)methoxy)(phenoxy)phosphoryl)amino)propanoate (4c).

Compound **4c** was prepared from **4a** by chiral chromatography. **4a** was dissolved in acetonitrile. The resulting solution was loaded onto Lux Cellulose-2 chiral column, equilibrated in acetonitrile, and eluted with isocratic acetonitrile/methanol (95:5 vol/vol). The first eluting

compound was the *R_p* diastereomer **4c**, and the second eluting compound was the *S_p* diastereomer **4b**.

¹H NMR (400 MHz, methanol-*d*₄) δ 8.05 (s, 1H), 7.36 (d, *J* = 4.8 Hz, 1H), 7.29 (br t, *J* = 7.8 Hz, 2H), 7.19 – 7.13 (m, 3H), 7.11 (d, *J* = 4.8 Hz, 1H), 4.73 (d, *J* = 5.2 Hz, 1H), 4.48 – 4.38 (m, 2H), 4.37 – 4.28 (m, 1H), 4.17 (t, *J* = 5.6 Hz, 1H), 4.08 – 3.94 (m, 2H), 3.94 – 3.80 (m, 1H), 1.48 (sep, *J* = 12.0, 6.1 Hz, 1H), 1.34 (p, *J* = 7.3 Hz, 4H), 1.29 (d, *J* = 7.2 Hz, 3H), 0.87 (t, *J* = 7.4 Hz, 6H). ³¹P NMR (162 MHz, methanol-*d*₄) δ 3.71 (s). MS *m/z* 603.1 [M+1].

(2*S*)-ethyl-2-((((2*R*,3*S*,4*R*,5*R*)-5-(4-aminopyrrolo[2,1-*f*][1,2,4]triazin-7-yl)-5-cyano-3,4-dihydroxytetrahydrofuran-2-yl)methoxy)(phenoxy)phosphoryl)amino)-3-phenylpropanoate (4d).

Compound **4** (0.030 g, 0.103 mmol) was dissolved in DMF (1 mL) and then THF (0.5 mL) was added. *t*-BuMgCl (1M/THF, 154.5 μL, 0.154 μmol) was added to the reaction in a drop-wise manner with vigorous stirring. The resulting white slurry was stirred at rt for about 30 min. A solution of compound **22d** (0.058 g, 0.124 mmol) in THF (1 mL) was added in a drop-wise manner to the reaction at rt. The reaction progress was monitored by LC/MS. When the reaction progressed to 50% conversion, the reaction was cooled in an ice bath and quenched with glacial acetic acid (70 μL). The reaction was concentrated and the crude residue was purified by reverse phase preparatory HPLC to afford compound **4d** (22 mg, 34%, as a 2.6:1 mixture of diastereomers at phosphorus). ¹H NMR (400 MHz, DMSO-*d*₆) δ 7.91 (d, *J* = 4 Hz, 1H), 7.90 (br s, 2H), 7.09-7.30 (m, 8H), 7.01, (t, *J* = 8.2 Hz, 2H), 6.89 (d, *J* = 4.4 Hz, 1H), 6.82 (t, *J* = 4.4 Hz, 1H), 6.27 (m, 1H), 6.14 (m, 1H), 5.34 (m, 1H), 4.62 (t, *J* = 5.6 Hz, 1H), 4.15 (m, 1H), 3.78-4.01 (m, 6H), 2.92 (m, 1H), 2.78 (m, 1H), 1.04 (m, 3H). ³¹P NMR (162 MHz, DMSO-*d*₆) δ 3.69 (s), 3.34 (s). MS *m/z* = 623.0 [M+1].

(2*S*)-ethyl-2-((((2*R*,3*S*,4*R*,5*R*)-5-(4-aminopyrrolo[2,1-*f*][1,2,4]triazin-7-yl)-5-cyano-3,4-dihydroxytetrahydrofuran-2-yl)methoxy)(phenoxy)phosphoryl)amino)-3-methylbutanoate (4e).

Compound **4** (0.040 g, 0.14 mmol) was dissolved in NMP (1.5 mL) and then THF (0.25 mL) was added. This solution was cooled in an ice bath and *t*-BuMgCl (1M/THF, 425.7 μL, 0.426 μmol)

was added in a drop-wise manner with vigorous stirring. The ice bath was removed and the resulting white slurry was stirred at rt for about 15 min. A solution of compound **22e** (0.081 g, 0.192 mmol) in THF (0.5 mL) was added in a drop-wise manner to the reaction at rt. The reaction progress was monitored by LC/MS. When the reaction progressed to 50% conversion, the reaction was cooled in an ice bath and quenched with glacial acetic acid (70 μ L). The reaction was concentrated and crude residue was semi-purified from the residue by reverse phase HPLC. The semi-pure material was further purified by silica gel column chromatography (eluent: 100% EtOAc ramping to 10% MeOH in EtOAc) to afford compound **4e** (0.034 g, 43% as a 1.8:1 mixture of diastereomers). ^1H NMR (400 MHz, DMSO- d_6) δ 7.91 (d, J = 1.6 Hz, 1H), 7.88 (br s, 2H), 7.32 (m, 2H), 7.15 (m, 3H), 6.90 (t, J = 4.2 Hz, 1H), 6.84 (d, J = 4.8 Hz, 1H), 6.26 (dd, J = 13.4, 6.2 Hz, 1H), 5.87 (q, J = 11.2 Hz, 1H), 5.35 (m, 1H), 4.64 (m, 1H), 4.25 (m, 2H), 3.93-4.15 (m, 4H), 3.45 (m, 1H), 1.87 (m, 1H), 1.09-1.16 (m, 3H), 0.70-0.83 (m, 6H). ^{31}P NMR (162 MHz, DMSO- d_6) δ 4.59 (s), 4.47 (s). MS m/z = 575.02 [M+1].

Ethyl 2-((((2*R*,3*S*,4*R*,5*R*)-5-(4-aminopyrrolo[2,1-*f*][1,2,4]triazin-7-yl)-5-cyano-3,4-dihydroxytetrahydrofuran-2-yl)methoxy)(phenoxy)phosphoryl)amino)-2-methylpropanoate (4f**).**

Compound **4** (66 mg, 0.23 mmol) was dissolved in NMP (2.0 mL) and the mixture was cooled to about 0 $^\circ\text{C}$. *t*-BuMgCl (1.0M in THF, 0.34 mL, 0.34 mmol) was then added and the resulting mixture was stirred at 0 $^\circ\text{C}$ for about 30 min. A solution of compound **22f** (139 mg, 0.34 mmol) in THF (1.0 mL) was then added, and the reaction mixture was heated to about 50 $^\circ\text{C}$. After about 2 h, the reaction was cooled to rt and quenched with acetic acid and methanol. The resulting mixture was concentrated under reduced pressure and purified by preparatory reverse phase HPLC to afford compound **4f** (32 mg, 25% as a 1.5:1 mixture of diastereomers). ^1H NMR (400 MHz, DMSO- d_6) δ 7.89 (m, 3H), 7.31 (q, J = 8.1 Hz, 2H), 7.22 – 7.05 (m, 3H), 6.87 (d, J = 4.5, 1H), 6.80 (d, J = 4.5 Hz, 1H), 6.27 (d, J = 11.7, 1H), 5.81 (d, J = 9.7, 1H), 5.35 (d, J = 5.6 Hz, 1H), 4.64 (dt, J = 9.0, 5.6 Hz, 1H), 4.24 (m, 2H), 4.11 (m, 1H), 4.04 – 3.90 (m, 3H), 1.39 – 1.23 (m, 6H), 1.10 (t, J = 7.1, 3H). ^{31}P NMR (162 MHz, DMSO- d_6) δ 2.45, 2.41. MS m/z = 561.03 [M+1].

Ethyl (((((2*R*,3*S*,4*R*,5*R*)-5-(4-aminopyrrolo[2,1-*f*][1,2,4]triazin-7-yl)-5-cyano-3,4-dihydroxytetrahydrofuran-2-yl)methoxy)(phenoxy)phosphoryl)-L-alaninate (4g).

Compound **4** (50 mg, 0.17 mmol) was dissolved in NMP-THF (1:1 mL)) and cooled with ice bath. *t*-BuMgCl (1.0M in THF, 0.257 mL, 0.257 mmol) was then added over about 5 min. The resulting mixture was allowed to warm to rt and was stirred for about 30 min. Then a solution of compound **22g** (74.6 mg, 0.189 mmol) in THF (2 mL) was added. After about 30 min, the reaction mixture was purified by preparatory reverse phase HPLC. Fractions containing the desired product were further purified with silica gel chromatography (eluent: 0-20% methanol in dichloromethane) to afford compound **4g** (23 mg, 24% as a 2.5:1 mixture of diastereomers). ¹H NMR (400 MHz, methanol-*d*₄) δ 7.76 (d, *J* = 6.0 Hz, 1H), 7.25 – 7.14 (m, 2H), 7.11 – 6.99 (m, 3H), 6.87 – 6.72 (m, 2H), 4.70 (d, *J* = 5.4 Hz, 1H), 4.39 – 4.24 (m, 2H), 4.20 (dddd, *J* = 9.7, 7.9, 5.1, 2.8 Hz, 1H), 4.10 (dt, *J* = 12.8, 5.5 Hz, 1H), 4.06 – 3.91 (m, 2H), 3.72 (ddq, *J* = 14.3, 9.3, 7.1 Hz, 1H), 1.17 (dd, *J* = 7.1, 1.0 Hz, 1H), 1.14 – 1.06 (m, 5H). ³¹P NMR (162 MHz, methanol-*d*₄) δ 3.73, 3.68. MS *m/z* = 547 [M+1].

Cyclopropylmethyl (((((2*R*,3*S*,4*R*,5*R*)-5-(4-aminopyrrolo[2,1-*f*][1,2,4]triazin-7-yl)-5-cyano-3,4-dihydroxytetrahydrofuran-2-yl)methoxy)(phenoxy)phosphoryl)-L-alaninate (4h).

To a mixture of compound **4** (60 mg, 0.21 mmol), compound **22h** (120 mg, 0.29 mmol), and MgCl₂ (29 mg, 0.31 mmol) in DMF (4 mL) was added *N,N*-diisopropylethylamine (0.09 mL, 0.52 mmol) dropwise at rt. The resulting mixture was stirred at 50 °C for 1h. The resulting mixture was concentrated under reduced pressure and the crude residue was purified by preparative reverse phase HPLC to afford compound **4h** (45 mg, 38%, 1:1.9 diastereomeric mixture). ¹H NMR (400 MHz, methanol-*d*₄) δ 7.85 (m, 1H), 7.28 (m, 2H), 7.24 – 7.10 (m, 3H), 6.99 – 6.80 (m, 2H), 4.79 (m, 1H), 4.50 – 4.23 (m, 3H), 4.25 – 4.13 (m, 1H), 3.97 – 3.74 (m, 3H), 1.26 (m, 3H), 1.08 (m, 1H), 0.50 (m, 2H), 0.24 (m, 2H). ³¹P NMR (162 MHz, methanol-*d*₄) δ 3.74, 3.62. MS *m/z* 573 [M+1].

(2*S*)-cyclobutyl 2-((((((2*R*,3*S*,4*R*,5*R*)-5-(4-aminopyrrolo[2,1-*f*][1,2,4]triazin-7-yl)-5-cyano-3,4-dihydroxytetrahydrofuran-2-yl)methoxy)(phenoxy)phosphoryl)amino)propanoate (4i).

Compound **4** (58 mg, 0.20 mmol) was mixed with compound **22i** (101 mg, 0.240 mmol) in 2 mL of anhydrous DMF. Magnesium chloride (42 mg, 0.44 mmol) was added in one portion. The

reaction mixture was heated to about 50 °C. *N,N*-Diisopropylethylamine (87 µL, 0.5 mmol) was added, and the reaction was stirred for about 2 h at about 50 °C. The reaction mixture was cooled to room temperature, was diluted with ethyl acetate and was washed with 5% aqueous citric acid solution followed by saturated aqueous sodium chloride solution. The organic layer was then dried over anhydrous sodium sulfate and concentrated under reduced pressure. The crude residue was purified with silica gel column (eluent: 0-5% methanol in dichloromethane) to afford compound **4i** (42 mg, 37% yield, as a 3:2 mixture of diastereomers). ¹H NMR (400 MHz, methanol-*d*₄) δ 7.85 (m, 1H), 7.34 – 7.22 (m, 2H), 7.22 – 7.08 (m, 3H), 6.94 – 6.84 (m, 2H), 4.95 – 4.85 (m, 1H), 4.79 (m, 1H), 4.46 – 4.34 (m, 2H), 4.34 – 4.24 (m, 1H), 4.19 (m, 1H), 3.81 (m, 1H), 2.27 (m, 2H), 2.01 (m, 2H), 1.84 – 1.68 (m, 1H), 1.62 (m, 1H), 1.30 – 1.16 (m, 3H). ³¹P NMR (162 MHz, methanol-*d*₄) δ 3.70, 3.65. MS *m/z* = 573.0 [M+1].

(*S*)-Isopropyl 2-(((*R*)-(((2*R*,3*S*,4*R*,5*R*)-5-(4-aminopyrrolo[2,1-*f*][1,2,4]triazin-7-yl)-5-cyano-3,4-dihydroxytetrahydrofuran-2-yl)methoxy)(phenoxy)phosphoryl)amino)propanoate (4j**).**

Compound **4** (60.0 mg, 206 µmol) was dissolved in NMP (0.28 mL). THF (0.2 mL) was added followed by *tert*-butyl magnesium chloride (1.0M solution in tetrahydrofuran, 0.309 mL) at rt under an argon atmosphere. After 20 min, a solution of compound **22j** (81 mg, 206 µmol) in THF (0.2 mL) was added, and the resulting mixture was warmed to about 50 °C. After 3 h, the reaction mixture was allowed to cool to rt and was purified directly by preparatory HPLC to afford compound **4j** (44 mg, 38% as a single diastereomer). ¹H NMR (400 MHz, methanol-*d*₄) δ 7.86 (s, 1H), 7.34 – 7.26 (m, 2H), 7.21 – 7.12 (m, 3H), 6.91 (d, *J* = 4.6 Hz, 1H), 6.87 (d, *J* = 4.6 Hz, 1H), 4.92 (septet, *J* = 6.3 Hz, 1H), 4.80 (d, *J* = 5.4 Hz, 1H), 4.43 – 4.34 (m, 1H), 4.33 – 4.24 (m, 1H), 4.18 (t, *J* = 5.6 Hz, 1H), 3.82 (dq, *J* = 9.7, 7.1 Hz, 2H), 1.27 (dd, *J* = 7.1, 1.0 Hz, 3H), 1.18 (dd, *J* = 6.3, 4.8 Hz, 6H). ³¹P NMR (162 MHz, methanol-*d*₄) δ 3.72 (s). MS *m/z* = 561.11 [M+1].

***tert*-Butyl (((((2*R*,3*S*,4*R*,5*R*)-5-(4-aminopyrrolo[2,1-*f*][1,2,4]triazin-7-yl)-5-cyano-3,4-dihydroxytetrahydrofuran-2-yl)methoxy)(phenoxy)phosphoryl)-L-alaninate (**4k**).**

To a mixture of intermediate **4** (80 mg, 0.28 mmol), intermediate **22k** (174 mg, 0.41 mmol), and MgCl₂ (39 mg, 0.41 mmol) in DMF (4 mL) was added *N,N*-diisopropylethylamine (0.12 mL, 0.69 mmol) dropwise at room temperature. The reaction mixture was stirred at 50 °C for 1 h and

was cooled to rt. The resulting mixture was concentrated under reduced pressure to approximately 2 mL volume and was purified by reverse phase preparative HPLC. Fractions containing the desired product were combined and further purified by silica gel column chromatography (eluent: 0-20% methanol in methylene chloride) to afford compound **4k** (51 mg, 32%, 1.5:1 diastereomeric mixture). ^1H NMR (400 MHz, methanol- d_4) δ 7.86 (s, 0.4H), 7.84 (s, 0.6H), 7.28 (m, 2H), 7.21 – 7.10 (m, 3H), 6.96 – 6.83 (m, 2H), 4.79 (m, 1H), 4.46 – 4.34 (m, 2H), 4.28 (m, 1H), 4.22 – 4.13 (m, 1H), 3.81 – 3.64 (m, 1H), 1.40 (m, 9H), 1.22 (m, 3H). ^{31}P NMR (162 MHz, methanol- d_4) δ 3.79 (s). MS m/z = 575 [M+1].

Cyclobutylmethyl (((((2R,3S,4R,5R)-5-(4-aminopyrrolo[2,1-f][1,2,4]triazin-7-yl)-5-cyano-3,4-dihydroxytetrahydrofuran-2-yl)methoxy)(phenoxy)phosphoryl)-L-alaninate (4l**).**

To a mixture of **4** (70 mg, 0.24 mmol) and **22l** (224 mg, 0.30 mmol) in DMF (2 mL) was added 1M *t*-BuMgCl in THF (0.24 mL, 0.24 mmol) dropwise at rt. After 1 h, additional 1M *t*-BuMgCl (0.24 mL, 0.24 mmol) was added dropwise. The reaction mixture was stirred at room temperature for 1 h, neutralized with AcOH, concentrated to approximately 2 mL volume and was purified by reverse phase preparative HPLC. Fractions containing desired product were combined and further purified by silica gel column chromatography (eluent: 0-20% methanol in methylene chloride) to afford compound **4l** (51 mg, 36%, 1.7:1 diastereomeric mixture mixture). ^1H NMR (400 MHz, methanol- d_4) δ 7.86 (s, 0.38H), 7.84 (s, 0.62H), 7.34 – 7.23 (m, 2H), 7.21 – 7.09 (m, 3H), 6.96 – 6.83 (m, 2H), 4.79 (d, J = 5.4 Hz, 1H), 4.48 – 4.33 (m, 2H), 4.29 (dddd, J = 8.3, 6.6, 5.2, 2.2 Hz, 1H), 4.19 (dt, J = 12.5, 5.5 Hz, 1H), 4.09 – 3.92 (m, 2H), 3.85 (ddd, J = 14.2, 9.3, 7.1 Hz, 1H), 2.57 (h, J = 7.7 Hz, 1H), 2.10 – 1.95 (m, 2H), 1.94 – 1.80 (m, 2H), 1.74 (tt, J = 9.0, 6.4 Hz, 2H), 1.28 (dd, J = 7.1, 1.1 Hz, 1H), 1.23 (dd, J = 7.2, 1.2 Hz, 2H). ^{31}P NMR (162 MHz, methanol- d_4) δ 3.71, 3.63. MS m/z = 587 [M+H].

Pentan-3-yl (((((2R,3S,4R,5R)-5-(4-aminopyrrolo[2,1-f][1,2,4]triazin-7-yl)-5-cyano-3,4-dihydroxytetrahydrofuran-2-yl)methoxy)(phenoxy)phosphoryl)-L-alaninate (4m**).**

To a mixture of compound **4** (80 mg, 0.28 mmol), **22m** (170 mg, 0.39 mmol), and MgCl_2 (39 mg, 0.41 mmol) in DMF (4 mL) was added *N,N*-diisopropylethylamine (0.12 mL, 0.69 mmol) dropwise at rt. The resulting mixture was stirred at 50 °C for 1 h, concentrated to approximately 2 mL volume and purified by reverse phase preparative HPLC to afford compound **4m** (68 mg,

42%, 1.5:1 diastereomeric mixture). ^1H NMR (400 MHz, methanol- d_4) δ 7.86 (s, 0.4 H), 7.85 (s, 0.6 H), 7.33 – 7.23 (m, 2H), 7.21 – 7.08 (m, 3H), 6.95 – 6.84 (m, 2H), 4.79 (m, 1H), 4.69 (m, 1H), 4.47 – 4.34 (m, 2H), 4.34 – 4.24 (m, 1H), 4.19 (m, 1H), 3.85 (m, 1H), 1.64 – 1.42 (m, 4H), 1.29 (dd, J = 7.0, 1.1 Hz, 1.1 H), 1.23 (dd, J = 7.2, 1.3 Hz, 1.9H), 0.91 – 0.76 (m, 6H). ^{31}P NMR (162 MHz, methanol- d_4) δ 3.71, 3.69. MS m/z = 589 [M+1].

(2S)-cyclopentyl 2-((((2R,3S,4R,5R)-5-(4-aminopyrrolo[2,1-f][1,2,4]triazin-7-yl)-5-cyano-3,4-dihydroxytetrahydrofuran-2-yl)methoxy)(phenoxy)phosphoryl)amino) propanoate (4n).

Compound **4** (100 mg, 0.34 mmol) was dissolved in THF (2 mL) and cooled under ice water bath. Then 1M *t*-BuMgCl (0.52 mL, 0.77 mmol) was added dropwise slowly. The resulting mixture was stirred for about 30 min at rt. Then compound **22n** (247 mg, 0.52 mmol) in THF (2 mL) was added over about 5 min and the resulting mixture was stirred for about 24 h at rt. The resulting mixture was diluted with ethyl acetate, cooled under ice-water bath, treated with aq NaHCO_3 (2 mL), washed with brine, dried with sodium sulfate, and concentrated under reduced pressure. The resulting mixture was purified by silica gel column chromatography (eluent: 0-20% methanol in dichloromethane) followed by reverse phase preparatory HPLC to afford compound **4n** (47 mg, 23% as a 27:1 mixture of diastereomers). ^1H NMR (400 MHz, methanol- d_4) δ 7.85 (s, 1H), 7.33 – 7.22 (m, 2H), 7.14 (tdd, J = 7.6, 2.1, 1.1 Hz, 3H), 6.95 – 6.87 (m, 2H), 5.13 – 5.00 (m, 1H), 4.78 (d, J = 5.4 Hz, 1H), 4.48 – 4.35 (m, 2H), 4.30 (ddd, J = 10.6, 5.7, 3.6 Hz, 1H), 4.19 (t, J = 5.4 Hz, 1H), 3.78 (dq, J = 9.2, 7.1 Hz, 1H), 1.81 (dtd, J = 12.5, 5.9, 2.4 Hz, 2H), 1.74 – 1.49 (m, 6H), 1.21 (dd, J = 7.1, 1.2 Hz, 3H). MS m/z = 587 [M+1].

2-ethylbutyl (((((2R,3S,4R,5R)-5-(4-aminopyrrolo[2,1-f][1,2,4]triazin-7-yl)-5-cyano-3,4-dihydroxytetrahydrofuran-2-yl)methoxy)(phenoxy)phosphoryl)-D-alaninate (4o).

Compound **21** (50 mg, 0.15 mmol) was dissolved in anhydrous tetrahydrofuran (5 mL) and stirred under atmospheric argon. Compound **22o** (75 mg, 0.17 mmol) was added followed by magnesium chloride (21 mg, 0.23 mmol), and the reaction was warmed to 50 °C and stirred for 30 min. *N,N*-diisopropylethylamine (65.0 μL , 0.375 mmol) was added dropwise, and the reaction mixture was stirred for 3 h at 50 °C. The reaction mixture was then cooled in an ice bath and 12N HCl(aq) (175 μL) was added dropwise. The ice bath was removed and the reaction

mixture was stirred at rt for 4 h. The reaction mixture was diluted with ethyl acetate (15 mL) and cooled in an ice bath. 1N NaOH(aq) was added slowly to give pH of 10. The organic layer was then washed with 5% aqueous sodium carbonate solution and then saturated aqueous sodium chloride solution. The organic layer was then dried over anhydrous sodium sulfate and concentrated under reduced pressure. The crude residue was purified with silica gel column chromatography (eluent: 0-10% methanol in dichloromethane) to afford compound **4o** (60 mg, 66% yield as a 1.1:1 diastereomeric mixture). ¹H NMR (400 MHz, methanol-*d*₄) δ 7.87 – 7.83 (m, 1H), 7.37 – 7.22 (m, 2H), 7.22 – 7.04 (m, 3H), 6.96 – 6.79 (m, 2H), 4.82 – 4.75 (m, 1H), 4.45 – 4.23 (m, 3H), 4.18 (m, 1H), 4.06 – 3.85 (m, 3H), 1.52 – 1.38 (m, 1H), 1.38 – 1.24 (m, 7H), 0.85 (m, 6H). ³¹P NMR (162 MHz, methanol-*d*₄) δ 3.87, 3.55. MS *m/z* = 603.1 [M+1].

(2*S*,2'*S*)-diethyl 2,2'-((((2*R*,3*S*,4*R*,5*R*)-5-(4-aminopyrrolo[1,2-*f*][1,2,4]triazin-7-yl)-5-cyano-3,4-dihydroxytetrahydrofuran-2-yl)methoxy)phosphoryl)bis(azanediyl) dipropanoate (4p).

Compound **4** (14.6 mg, 0.05 mmol) was dissolved in anhydrous trimethyl phosphate (0.5 mL) and stirred under N₂(g) at rt. POCl₃ (9.2 μL, 0.1 mmol) was added and the mixture stirred for about 60 min. Alanine ethyl ester hydrochloride **18b** (61 mg, 0.4 mmol) and then Et₃N (70 μL, 0.5 mmol) was added. The resultant mixture was stirred for about 15 min. and then additional Et₃N (70 μL, 0.5 mmol) was added to give a solution pH of 9-10. The mixture was stirred for about 2 h. and then diluted with ethyl acetate, washed with saturated aqueous NaHCO₃ solution followed by saturated aqueous NaCl solution. The organic layer was dried over anhydrous sodium sulfate and concentrated under reduced pressure. The residue was purified by reverse phase preparative HPLC to afford compound **4p** (5.5 mg, 16%). ¹H NMR (400 MHz, methanol-*d*₄) δ 8.13 (s, 1H), 7.41 (d, *J* = 4.8 Hz, 1H), 7.18 (d, *J* = 4.8 Hz, 1H), 4.78 (d, *J* = 5.6 Hz, 1H), 4.36 (m, 1H), 4.25-4.08 (m, 7H), 3.83 (m, 2H), 1.33-1.23 (m, 12H). ³¹P NMR (121.4 MHz, methanol-*d*₄) δ 13.8. MS *m/z* 570.0 [M+1].

(2*S*,2'*S*)-di(2-ethylbutyl) 2,2'-((((2*R*,3*S*,4*R*,5*R*)-5-(4-aminopyrrolo[1,2-*f*][1,2,4]triazin-7-yl)-5-cyano-3,4-dihydroxytetrahydrofuran-2-yl)methoxy)phosphoryl)bis(azanediyl) dipropanoate (4q).

To a suspension of compound **4** (52 mg, 0.18 mmol) and solid sodium bicarbonate (53 mg) in trimethyl phosphate (1.5 mL) at 0 °C was added POCl₃ (120 mg, 0.783 mmol). The mixture was

stirred at 0 °C for 3 h, at which point a solution of **18a** (790 mg, 4.56 mmol) in MeCN (1 mL) was then added. The reaction mixture was stirred at 0 °C for 0.5 h, then triethylamine (0.1 mL) was added and stirred at rt for 0.5 h. The reaction mixture was diluted with ethyl acetate (10 mL), washed with water (10 mL), and was concentrated under reduced pressure. The residue was purified by silica gel column chromatography (eluent: 50-100% ethyl acetate in hexanes gradient followed by 0-10% methanol in ethyl acetate gradient) to afford compound **4q** (71 mg, 58%). ¹H NMR (400 MHz, methanol-*d*₄): δ 7.88 (s, 1H), 6.95 (d, *J* = 4.8 Hz, 1H), 6.89 (d, *J* = 4.4 Hz, 1H), 4.85 (d, *J* = 5.6 Hz, 1H), 4.32-4.35 (m, 1H), 4.12-4.26 (m, 3H), 4.04-4.09 (m, 2H), 3.94-3.98 (m, 2H), 3.79-3.89 (m, 2H), 1.44-1.54 (m, 2H), 1.27-1.39 (m, 14H), 0.89 (t, *J* = 7.2 Hz, 12H). ³¹P NMR (400 MHz, methanol-*d*₄): δ 13.83. MS *m/z* = 682.1 [M+1].

Supporting Information: Assay Methods, Molecular Modeling with RSV, Marburg and Sudan viruses, compound synthesis and single crystal X-Ray structure information are available in Supporting Information.

Accession Codes: The Cambridge Crystallographic Data Center (CCDC) numbers for the X-Ray structures of compound **22b** is 1445315. Authors will deposit the X-Ray structure of **4b** upon article publication.

Homology models: HIV (1RTD32b) and HCV (4WTG32c) X-Ray structures were used to generate the EBOV model for **4-TP** and **13-TP**. Authors will release the atomic coordinates upon article publication.

Acknowledgement: We acknowledge the contributions of the following individuals at USAMRIID for participation in vivo studies, J. Wells, K. Stuthman, N. Lackemeyer, S. Van Tongeren, G. Donnelly, J. Steffens, A. Shurtleff, L. Gomba, J. Benko; scientific input, L. Welch,

T. Bocan, A. Duplantier, R. Panchal, C. Kane, D. Mayers (currently of Cocrystal Pharma, Inc.); and for services performed, S Tritsch, C. Retterer, D. Gharaibeh, T. Kenny, B. Eaton, G. Gomba, J. Nuss and C. Rice. From Gilead Sciences we acknowledge K. Wang, K. Brendza, T. Alfredson and L. Serafini who assisted with analytical methods, S. Bondy and R. Seemayer procured key raw materials, L. Heumann, R. Polniaszeck, E. Rueden, A. ChtChemelinine, K. Brak and B. Hoang contributed to synthesis, and Yelena Zhrebina to chiral separations. These studies were in part supported by The Joint Science and Technology Office for Chemical and Biological Defense (JSTO-CBD) of the Defense Threat Reduction Agency (DTRA) under plan #CB10218. CDC core funding supported the work done by MKL at CDC

Disclaimer: Opinions, interpretations, conclusions, and recommendations are those of the authors and are not necessarily endorsed by the U.S. Army, U.S. Department of Health and Human Services, the Public Health Service, the Centers for Disease Control and Prevention, or the authors' affiliated institutions. Research was conducted under an IACUC approved protocol in compliance with the Animal Welfare Act, PHS Policy, and other Federal statutes and regulations relating to animals and experiments involving animals. The facility where this research was conducted is accredited by the Association for Assessment and Accreditation of Laboratory Animal Care, International and adheres to principles stated in the Guide for the Care and Use of Laboratory Animals, National Research Council, 2011.

Abbreviations Used: EBOV, Ebola virus; EVD, Ebola virus disease; USAMRIID, United States Army Medical Research Institute of Infectious Diseases; SARS, severe acute respiratory

syndrome; MERS, Middle East respiratory syndrome; BSL-4, Biosafety Level 4; HMVECTERT; human foreskin microvascular endothelial cells; RSV, respiratory syncytial virus; HEp-2, Human epithelial type 2 cell; Huh-7, Hepatocellular carcinoma cell; MT4, Human leukemia Tcell; Pol, polymerase; NTP, nucleoside triphosphate; POLRMT, mitochondrial RNA polymerase; SNI, single nucleotide incorporation; NMI, *N*-methyl imidazole; PNP, *para*-nitrophenol; PFP, pentafluorophenol; LG, leaving group; LogD, logarithm of distribution coefficient; Macro, human macrophage cells; NHP, nonhuman primate; IND, investigational new drug; SD, standard deviation; PBMC, peripheral blood mononuclear cell; IACUC, Institutional Animal Care and Use Committee.

References

1. World Health Organization. *Ebola Situation Report - 10 June 2016*.
http://apps.who.int/iris/bitstream/10665/208883/1/ebolasitrep_10Jun2016_eng.pdf?ua=1
 (accessed July 22, 2016).
2. World Health Organization. *Ebola Data and Statistics – 11 May 2016*.
<http://apps.who.int/gho/data/view ebola-sitrep ebola-summary-20160511?lang=en>
 (accessed July 22, 2016).
3. Vetter, P.; Fischer, W. A. II; Schibler, M.; Jacobs, M.; Baushc, D. G.; Kaiser, L. Ebola Virus Shedding and Transmission: Review of Current Evidence. *J. Infect. Dis.* **2016**, S1-S8.
4. Mate, S. E.; Kugelman, J. R.; Nyenswah, T. G.; Ladner, J. T.; Wiley, M. R.; Cordier-Lassalle, T.; Christie, A.; Schroth, G. P.; Gross, S. M.; Davies-Wayne, G. J.; Shinde, S. A.; Murugan, R.; Sieh, S. B.; Badio, M.; Fakoli, L.; Taweh, F.; de Wit, E.; van Doremalen, N.; Munster, V. J.; Pettitt, J.; Prieto, K.; Humrighouse, B. W.; Ströher, U.; DiClaro, J. W.; Hensley, L. E.; Schoepp, R. J.; Safronetz, D.; Fair, J.; Kuhn, J. H.; Blackley, D. J.; Laney, A. S.; Williams, D. E.; Lo, T.; Gasasira, A.; Nichol, S. T.; Formenty, P.; Kateh, F. N.; De Cock, K. M.; Bolay, F.; Sanchez-Lockhart, M.; Palacios,

- G. Molecular Evidence of Sexual Transmission of Ebola Virus. *N. Engl. J. Med.* **2015**, 373, 2448-2454.
5. Kuhn, J. H. Filoviruses: A Compendium of 40 Years of Epidemiological, Clinical, and Laboratory Studies. (SpringWien, New York, 2008).
6. Rougeron, V.; Feldmann, H.; Grard, G.; Becker, S.; Leroy, E. M. Ebola and Marburg haemorrhagic fever. *J. Clin. Virol.* **2015**, 64, 111-119.
7. Qiu, X.; Wong, G.; Audet, J.; Bello, A.; Fernando, L.; Alimonti, J. B.; Fausther-Bovendo, H.; Wei, H.; Aviles, J.; Hiatt, E.; Johnson, A.; Morton, J.; Swope, K.; Bohorov, O.; Bohorova, N.; Goodman, C.; Kim, D.; Pauly, M. H.; Velasco, J.; Pettitt, J.; Olinger, G. G.; Whaley, K.; Xu, B.; Strong, J. E.; Zeitlin, L.; Kobinger, G. P. Reversion of Advanced Ebola Virus Disease in Nonhuman Primates with ZMapp. *Nature* **2014**, 514, 47-53.
8. Thi, E. P.; Mire, C. E.; Lee, A. C. H.; Geisbert, J. B.; Zhou, J. Z.; Agans, K. N.; Snead, N. M.; Deer, D. J.; Barnard, T. R.; Fenton, K. A.; MacLachlan, I.; Geisbert, T. W. Lipid Nanoparticles siRNA Treatment of Ebola-Virus-Makona-Infected Nonhuman Primates. *Nature* **2015**, 521, 362-365.
9. Tekmira Pharmaceuticals Corporation. *Tekmira Provides Update on TKM-Ebola-Guinea.* <http://www.sec.gov/Archives/edgar/data/1447028/000117184315003522/newsrelease.htm> (2015) (accessed July 22, 2016).
10. Iversen, P. L.; Warren, T. K.; Wells, J. B.; Garza, N. L.; Mourich, D. V.; Welch, L. S.; Panchal, R. G.; Bavari, S. Discovery and Early Development of AVI-7537 and AVI-7288 for the Treatment of Ebola Virus and Marburg Virus Infections. *Viruses* **2012**, 4, 2806-2830.
11. Oestereich, L.; Lüdtke, A.; Wurr, S.; Rieger, T.; Muñoz-Fontela, C.; Günther, S. Successful Treatment of Advanced Ebola Virus Infection with T-705 (favipiravir) in a Small Animal Model. *Antiviral Res.* **2014**, 105, 17-21.
12. Smither, S. J.; Eastaugh, L. S.; Steward, J. A.; Nelson, M.; Lenk, R. P.; Lever, M. S. Post-exposure efficacy of Oral T-705 (Favipiravir) Against Inhalational Ebola Virus Infection in a Mouse Model. *Antiviral Res.* **2014**, 104, 153-155.
13. Sissoko, D.; Folkesson, E.; Abdoul, M.; Beavogui, A. H.; Gunther, S.; Shepherd, S.; Danel, C.; Mentre, F.; Anglaret, X.; Malvy, D. Favipiravir in Patients with Ebola Virus Disease: Early Results of the JIKI trial in Guinea, CROI Conference, Boston, MA, Feb

- 22–25, 2016. [Abstract 103-ALB]. *Conference of Retroviruses and Opportunistic Infections (CROI)* (Seattle, WA, 2015).
14. McMullan, L. K.; Flint, M.; Dyall, J.; Albariño, C.; Olinger, G. G.; Foster, S.; Sethna, P.; Hensley, L. E.; Nichol, S. T.; Lanier, E. R.; Spiropoulou, C. F. The Lipid Moiety of Brincidofovir is Required for In Vitro Antiviral Activity Against Ebola Virus. *Antiviral Res.* **2016**, *125*, 71-78.
 15. Warren, T. K.; Wells, J.; Panchal, R. G.; Stuthman, K. S.; Garza, N. L.; Van Tongeren, S. A.; Dong, L.; Retterer, C. J.; Eaton, B. P.; Pegoraro, G.; Honnold, S.; Bantia, S.; Kotian, P.; Chen, X.; Taubenheim, B. R.; Welch, L. S.; Minning, D. M.; Babu, Y. S.; Sheridan, W. P.; Bavari, S. Protection Against Filovirus Disease by a Novel Broad-Spectrum Nucleoside Analogue BCX4430. *Nature* **2014**, *508*, 402-405.
 16. Henao-Restrepo, A. M.; Longini, I. M.; Egger, M.; Dean, N. E.; Edmunds, W. J.; Camacho, A.; Carroll, M. W.; Doumbia, M.; Draguez, B.; Duraffour, S.; Enwere, G.; Grais, R.; Gunther, S.; Hossmann, S.; Kondé, M. K.; Kone, S.; Kuisma, E.; Levine, M. M.; Mandal, S.; Norheim, G.; Riveros, X.; Soumah, A.; Trelle, S.; Vicari, A. S.; Watson, C. H.; Kéïta, S.; Kieny, M. P.; Røttingen, J.-A. Efficacy and Effectiveness of an rVSV-Vectored Vaccine Expressing Ebola, Surface Glycoprotein: Interim Results from the Guinea Ring Vaccination Cluster-Randomised Trial. *Lancet* **2015**, *386*, 857-866.
 17. Warren, T. K.; Jordan, R.; Lo, M. K.; Ray, A. S.; Mackman, R. L.; Soloveva, V.; Siegel, D.; Perron, M.; Bannister, R.; Hui, H. C.; Larson, N.; Strickley, R.; Wells, J.; Stuthman, K. S.; Van Tongeren, S. A.; Garza, N. L.; Donnelly, G.; Shurtleff, A. C.; Retterer, C. J.; Gharaibeh, D.; Zamani, R.; Kenny, T.; Eaton, B. P.; Grimes, E.; Welch, L. S.; Gomba, L.; Wilhelmsen, C. L.; Nichols, D. K.; Nuss, J. E.; Nagle, E. R.; Kugelman, J. R.; Palacios, G.; Doerffler, E.; Neville, S.; Carra, E.; Clarke, M. O.; Zhang, L.; Lew, W.; Ross, B.; Wang, Q.; Chun, K.; Wolfe, L.; Babusis, D.; Park, Y.; Stray, K. M.; Trancheva, I.; Feng, J. Y.; Barauskas, O.; Xu, Y.; Wong, P.; Braun, M. R.; Flint, M.; McMullan, L. K.; Chen, S. S.; Fearn, R.; Swaminathan, S.; Mayers, D. L.; Spiropoulou, C. F.; Lee, W. A.; Nichol, S. T.; Cihlar, T.; Bavari, S. Therapeutic Efficacy of the Small Molecule GS-5734 Against Ebola Virus in Rhesus Monkeys. *Nature* **2016**, *531*, 381-385.

18. Mehellou, Y.; Balzarini, J.; McGuigan, C. Aryloxy Phosphoramidate Triesters: a Technology for Delivering Monophosphorylated Nucleosides and Sugars into Cells. *Chem. Med. Chem.* **2009**, *4*, 1779-1791.
19. Sofia, M. J. Bao, D.; Chang, W.; Du, J.; Nagarathnam, D.; Rachakonda, S.; Reddy, P. G.; Ross, B. S.; Wang P.; Zhang, H.-R.; Bansal, S.; Espiritu, C.; Keilman, M.; Lam, A. M.; Micolochick Steuer, H. M.; Niu, C.; Otto, M. J.; Furman, P. A. Discovery of a β -D-2'-Deoxy-2'- α -fluoro-2'- β -C-methyluridine Nucleotide Prodrug (PSI-7977) for the Treatment of Hepatitis C Virus. *J. Med. Chem.* **2010**, *53*, 7202-7218.
20. Lee, A. W.; He, G.-X.; Eisenberg, E.; Cihlar, T.; Swaminathan, S.; Mulato, A.; Cundy, K. C. Selective Intracellular Activation of a Novel Prodrug of the Human Immunodeficiency Virus Reverse Transcriptase Inhibitor Tenofovir Leads to Preferential Distribution and Accumulation in Lymphatic Tissue. *Antimicrob. Agents Chemother.* **2005**, *49*, 1898-1906.
21. Murakami, E.; Niu, C.; Bao, H.; Micolochick Steuer, H. M.; Whitaker, T.; Nachman, T.; Sofia, M. A.; Wang, P.; Otto, M. J.; Furman, P. A. The Mechanism of Action of β -D-2'-Deoxy-2'-Fluoro-2'-C-Methylcytidine Involves a Second Metabolic Pathway Leading to β -D-2'-Deoxy-2'-Fluoro-2'-C-Methyluridine 5'-Triphosphate, a Potent Inhibitor of the Hepatitis C Virus RNA-Dependent RNA Polymerase. *Antimicrob. Agents Chemother.* **2008**, *52*, 458-464.
22. Cho, A.; Suanders, O. L.; Butler, T.; Zhang, L.; Xu, J.; Vela, J. E.; Feng, J. Y.; Ray, A. S.; Kim, C. U. Synthesis and Antiviral Activity of a Series of 1'-Substituted 4-aza-7,9-dideazaadenosine C-nucleosides. *Bioorg. Med. Chem. Lett.* **2012**, *22*, 2705-2707.
23. Mackman, R. L.; Parrish, J. P.; Ray, A. S.; Theodore, D. A. Methods and Compounds for Treating Paramyxoviridae Virus Infections. U.S. Patent 2011045102 July, 22, 2011.
24. Patil, S. A.; Otter, P. B.; Klein, R. S. 4-Aza-7,9-dideazaadenosine, a New Cytotoxic Synthetic C-Nucleoside Analogue of Adenosine. *Tetrahedron Lett.* **1994**, *35*, 5339-5342.
25. Chen, G.; Lou, Z.; Xie, Y. Cyanoribofuranoside Compound and Its Preparing Method. Chinese Patent CN1137132C February, 4, 2004.
26. Yoshimura, Y.; Kano, F.; Miyazaki, S.; Ashida, N.; Sakata, S. Synthesis and Biological Evaluation of 1'-C-cyano-pyrimidine nucleosides. *Nucleosides Nucleotides.* **1996**, *15*, 305-324.

27. Kirschberg, T. A.; Mish, M.; Squires, N. H.; Zonte, S.; Aktoudianakis, E.; Metobo, S.; Butler, T.; Ju, X.; Cho, A.; Ray, A. S.; Kim, C. U. Synthesis of 1'-C-Cyano Pyrimidine Nucleosides and Characterization as HCV Polymerase Inhibitors. *Nucleosides, Nucleotides and Nucleic Acids*, **2015**, 34, 763-785.
28. Clarke, M. O.; Mackman, R.; Byun, D.; Hui, H.; Barauskas, O.; Birkus, G.; Chun, B.-K.; Doerffler, E.; Feng, J.; Karki, K.; Lee, G.; Perron, M.; Siegel, D.; Swaminathan, S.; Lee, W. Discovery of β -D-2'- α -fluoro-4'- α -cyano-5-aza-7,9-dideaza Adenosine As A Potent Nucleoside Inhibitor of Respiratory Syncytial Virus, with Excellent Selectivity over Mitochondrial RNA and DNA Polymerases. *Bioorg. Med. Chem. Lett.* **2015**, 25, 2484-2487.
29. Feng, J.; Xu, Y.; Barauskas, O.; Perry, J. K.; Ahmadyar, S.; Stepan, G.; Yu, H.; Babusis, D.; Park, Y.; McCutcheon, K.; Perron, M.; Schultz, B. E.; Sakowicz, R.; Ray, A. S. Role of Mitochondrial RNA Polymerase in the Toxicity of Nucleotide Inhibitors of Hepatitis C Virus. *Antimicrob. Agents Chemother.* **2016**, 60, 806-817.
30. Bouloy, M.; Bishop, D. H. L.; Delarue, M.; Poch, O.; Müller, R. Rift Valley Fever Virus L Segment: correction of the sequence and possible functional role of newly identified regions conserved in RNA-dependent polymerases. *J. Gen Virol*, **1994**, 75, 1345-1352.
31. For alignments see the supplementary information.
32. Feng, J. Y.; Cheng, G.; Perry, J.; Barauskas, O.; Xu, Y.; Fenaux, M.; Eng, S.; Tirunagari, N.; Peng, B.; Yu, M.; Tian, Y.; Lee, Y.-J.; Stepan, G.; Lagpacan, L. L.; Jin, D.; Hung, M.; Ku, K. S.; Han, B.; Kitrinis, K.; Perron, M.; Birkus, G.; Wong, K. A.; Zhong, W.; Kim, C. U.; Carey, A.; Cho, A.; Ray, A. S. Inhibition of Hepatitis C Virus Replication by GS-6620, a Potent, C-Nucleoside Monophosphate Prodrug. *Antimicrob. Agents Chemother.* **2014**, 58, 1930-1942.
33. Butler, T.; Cho, A.; Kim, C. U.; Saunders, O. L.; Zhang, L. 1'-Substituted Carba-nucleoside Analogues for Antiviral treatment. U.S. Patent 2009041447 April, 22, 2009.
34. Butler, T.; Cho, A.; Graetz, B. R.; Kim, C. U.; Metobo, S. E.; Saunders, O. L.; Waltman, A. W.; Xu, J.; Zhang, L. Processes and Intermediates for the Preparation of 1'-substituted Carba-nucleoside Analogues. U.S. Patent 20100459508 September, 20, 2010.

35. Metobo, S. E.; Xu, J.; Saunders, O. L.; Butler, T.; Aktoudianakis, E.; Cho, A.; Kim, C. U. Practical Synthesis of 1'-Substituted Tubercidin C-Nucleoside Analogs. *Tetrahedron Lett.* **2012**, 53, 484-486.
36. Axt, S. D.; Badalov, P. R.; Brak, K.; Campagna, S.; Chtchemelinine, A.; Chun, B. K.; Clarke, M. O. H.; Doerffler, E.; Frick, M. M.; Gao, D.; Heumann, L. V.; Hoang, B.; Hui, H. C.; Jordan R.; Lew, W.; Mackman, R. L.; Milburn, R. R.; Neville, S. T.; Parrish, J. P.; Ray, A. S.; Ross, B.; Rueden, E.; Scott, R. W.; Siegel, D.; Stevens, A. C.; Tadeus, C.; Vieira, T.; Waltman, A. W.; Wang, X.; Whitcomb, M. C.; Wolfe, L.; Yu, C.-Y. Methods for Treating Filoviridae Virus Infections. U.S. Patent 2015017934, October 29, 2015.
37. Krasovskiy, A.; Knochel, P. A LiCl-Mediated Br/Mg Exchange Reaction for the Preparation of Functionalized Aryl- and Heteroarylmagnesium Compounds from Organic Bromides. *Angew. Chem. Int. Ed.*, **2004**, 43, 3333-3336.
38. For a separate account describing the crystallization induced resolution of *p*-nitrophenolate 2-ethylbutyl-L-alaninate phosphoramidate see: Klasson, B.; Eneroth, A.; Nilson, M.; Pinho, P.; Samuelsson, B.; Sund, C. HCV Polymerase Inhibitors. European Patent IB2012056994 December 5, 2012. The conditions in this manuscript were identified independently/concurrently with this report.
39. Bahar, F. G.; Ohura, K.; Ogihara, T.; Imai, T. Species Difference of Esterase Expression and Hydrolase Activity in Plasma. *J. Pharm. Sci.* **2012**, 101, 3979-3988.
40. Jacobs, M.; Rodger, A.; Bell, D. D.; Bhagani, S.; Cropley, I.; Filipe, A.; Gifford, R. J.; Hopkins, S.; Hughes, J.; Jabeen, F.; Johannessen, I.; Karageorgopoulos, D.; Lackenby, A.; Lester, R.; Liu, R. S. N.; MacConnachie, A.; Mahungu, T.; Martin, D.; Marshall, N.; Mephram, S.; Orton, R.; Pamarini, M.; Patel, M.; Perry, C.; Peters, S. E.; Porter, D.; Ritchie, D.; Ritchie, N. D.; Seaton, R. A.; Sreenu, V. B.; Templeton, K.; Warren, S.; Wilkie, G. S.; Zambon, M.; Gopal, R.; Thomson, E. C. Late Ebola Virus Relapse Causing Meningoencephalitis: A Case Report. *Lancet*, **2016**, 388, 498-503.
41. Schnirring, L. Center for Infectious Disease Research and Policy. Youngest Ebola Survivor Leaves Guinea Hospital. <http://www.cidrap.umn.edu/news-perspective/2015/11/youngest-ebola-survivor-leaves-guinea-hospital>, November 30, 2015 (accessed July 22, 2016).

42. National Institutes of Health. PREVAIL Treatment Trial for Men with Persistent Ebola Viral RNA in Semen Opens in Liberia. <https://www.nih.gov/news-events/news-releases/prevail-treatment-trial-men-persistent-ebola-viral-rna-semen-opens-liberia>, July 5, 2016. (accessed, July, 22, 2016).

Supporting Information

General Information

Comment [DS1]: Things to be done
 1)Deposit X-ray in Database
 2)POLMRT vs mtRNA
 3)Modeling Additions – Jason Perry.

Viruses

RSV A2 was purchased from Advanced Biotechnologies, Inc. HCV subgenomic replicon Genotype 1b-Con1 was generated as described previously.^{1,2} EBOV (Kikwit) were prepared and characterized at USAMRIID. EBOV containing a GFP reporter gene (EBOV-GFP) was prepared and characterized at the Centers for Disease Control and Prevention (CDC).^{3,4}

Cells

HEp-2 (CCL-23), and HeLa (CCL-2) cell lines were purchased from the American Type Culture Collection. Cell lines were not authenticated and were not tested for mycoplasma as part of routine use in assays. HEp-2 cells were cultured in Eagle's Minimum Essential Media (MEM) with GlutaMAXTM supplemented with 10% fetal bovine serum (FBS) and 100 units/mL penicillin and streptomycin. HeLa cells were cultured in MEM supplemented with 10% FBS, 1% l-glutamine, 10 mM HEPES, 1% non-essential amino acids, and 1% penicillin/streptomycin. The MT-4 cell line was obtained from the NIH AIDS Research and Reference Reagent Program and cultured in RPMI-1640 medium supplemented with 10% FBS, 100 units/mL penicillin and streptomycin, and 2 mM l-glutamine. The Huh-7 cell line was obtained from Dr. Charles M. Rice at the Rockefeller University and cultured in DMEM supplemented with 10% FBS, 100 units/mL penicillin and streptomycin, and non-essential amino acids. Human peripheral blood mononuclear cells (PBMCs) were isolated from human buffy coats obtained from healthy volunteers (Stanford Medical School Blood Center, Palo Alto, CA) and maintained in RPMI-1640 with GlutaMAXTM supplemented with 10% FBS, 100 units/mL penicillin and streptomycin. Human macrophage cultures were isolated from PBMCs that were purified by Ficoll gradient centrifugation from 50 mL of blood from healthy human volunteers. PBMCs were cultured for 7 to 8 days in in RPMI cell culture media supplemented with 10% FBS, 5 to 50 ng/mL granulocyte-macrophage colony-stimulating factor (GM-CSF) and 50 μ M β -mercaptoethanol (BME) to induce macrophage differentiation. Immortalized human

microvascular endothelial cells (HMVEC-TERT) were obtained from Dr. Rong Shao at the Pioneer Valley Life Sciences Institute²⁸. HMVEC-TERT cells were cultured in endothelial basal media supplemented with 10% FBS, 5 µg of epithelial growth factor, 0.5 mg hydrocortisone, and gentamycin/amphotericin-B. Normal human bronchial epithelial (NHBE) cells were purchased from Lonza (Walkersville, MD, Cat # CC-2540) and cultured in Bronchial Epithelial Growth Media (BEGM) (Lonza, Walkersville, MD, Cat # CC-3170). The cells were passaged 1-2 times per week to maintain < 80% confluency. The NHBE cells were discarded after 6 passages in culture.

EBOV HMVEC Antiviral Assay

Antiviral assays were conducted in biosafety level-4 containment (BSL-4) at the CDC. HMVEC-TERT cells were seeded in 96 well plates. Eight to ten concentrations of compound were diluted in 3-fold serial dilution increments in media and 100 µL/well of each dilution was transferred in triplicate onto 96 well plates containing preseeded HMVEC-TERT monolayers. The plates were transferred to BSL-4 containment and the appropriate dilution of EBOV-GFP virus stock, previously determined by titration and prepared in cell culture media, was added to test plates containing cells and serially diluted compounds. Each plate included three wells of infected untreated cells and three wells of uninfected cells that served as 0% and 100% virus inhibition control, respectively. Following the infection, test plates were incubated for 3 to 4 days in a tissue culture incubator. After the incubation, virus replication was measured in an Envision plate reader by direct fluorescence to measure GFP expression from the reporter virus. The percentage inhibition was calculated for each tested concentration relative to the 0% and 100% inhibition controls and the EC₅₀ value for each compound was determined by non-linear regression as the effective concentration of compound that inhibited virus replication by 50%.

EBOV HeLa Antiviral Assay

The antiviral activity of selected compounds was measured against EBOV (Kikwit) conducted in BSL-4 at the US Army Medical Research Institute for Infectious Disease (USAMRIID). HeLa cells were seeded in 384 well plates at 5000 cells / well. The antiviral activity of each compound was measured in quadruplicate. Eight to ten concentrations of compound were added directly to the cell cultures using the HP300 digital dispenser in 3-fold serial dilution increments 2h prior to

infection. The plates were transferred to BSL-4 containment and the appropriate dilution of virus stock, previously determined by titration and prepared in cell culture media, was added to test plates containing cells and serially diluted compounds. Each plate included three wells of infected untreated cells and three wells of uninfected cells that served as 0% and 100% virus inhibition control, respectively. Following the infection, test plates were incubated for 2 days in a tissue culture incubator. After the incubation, the cells were fixed in formalin solution and virus replication was measured by quantifying Ebola glycoprotein levels after immunostaining and high content imaging using the Perkin Elmer Opera confocal microscopy instrument. The percentage inhibition was calculated for each tested concentration relative to the 0% and 100% inhibition controls and the EC₅₀ value for each compound was determined by non-linear regression as the effective concentration of compound that inhibited virus replication by 50%.

EBOV Human Macrophage Antiviral Assay

The antiviral activity was measured against EBOV (Kikwit) conducted in BSL-4 USAMRIID. Macrophage cultures were isolated from fresh human PBMCs and differentiated in the presence of 5ng/ml GM-CSF and 50uM B-mercaptoethanol. The media was changed every 2 days and cells that adhered to the tissue culture plate after 7 days were removed with 0.5M EDTA in 1x PBS, concentrated by centrifugation at 200 x g for 10 minutes and plated in 384 well assay plates at 40,000 cells / well. The antiviral activity of each compound was measured in quadruplicate. Eight to ten concentrations of compound were added directly to the cell cultures using the HP300 digital dispenser in 3-fold serial dilution increments 2h prior to infection. The plates were transferred to BSL-4 containment and the appropriate dilution of virus stock, previously determined by titration and prepared in cell culture media, was added to test plates containing cells and serially diluted compounds. Each plate included three wells of infected untreated cells and three wells of uninfected cells that served as 0% and 100% virus inhibition control, respectively. Following the infection, test plates were incubated for 2 days in a tissue culture incubator. After the incubation, the cells were fixed in formalin solution and virus replication was measured by quantifying Ebola glycoprotein levels after immunostaining and high content imaging using the Perkin Elmer Opera confocal microscopy instrument. The percentage inhibition was calculated for each tested concentration relative to the 0% and 100% inhibition

controls and the EC₅₀ value for each compound was determined by non-linear regression as the effective concentration of compound that inhibited virus replication by 50%.

RSV A2 HEp-2 Antiviral Assay

Compounds were 3-fold serially diluted in source plates from which 100 nL of diluted compound was transferred to a 384-well cell culture plate using an Echo acoustic transfer apparatus. HEp-2 cells at a density of 5×10^5 cells/mL were then infected by adding RSV A2 at a titer of $1 \times 10^{4.5}$ tissue culture infectious doses (TCID₅₀)/mL. Immediately following virus addition, 20 µL of the virus/cell mixture was added to the 384-well cell culture plates using a µFlow liquid dispenser and cultured for 4 days at 37 °C. After incubation, the cells were allowed to equilibrate to 25 °C for 30 minutes. The RSV-induced cytopathic effect was determined by adding 20 µL of CellTiter-Glo™ Viability Reagent. After a 10-minute incubation at 25 °C, cell viability was determined by measuring luminescence using an Envision plate reader.

RSV A2 NHBE Antiviral Assay

NHBE cells were plated in 96-well plates at a density of 7,500 cells per well in BEGM and allowed to attach overnight at 37°C. Following attachment, 100 µL of cell culture media was removed and 3-fold serially diluted compound was added using a Hewlett-Packard D300 Digital Dispenser. The final concentration of DMSO was normalized to 0.05%. Following compound addition, the NHBE cells were infected by the addition of 100 µL of RSV A2 at a titer of $1 \times 10^{4.5}$ tissue culture infectious doses/mL in BEGM and then incubated at 37 °C for 4 days. The NHBE cells were then allowed to equilibrate to 25 °C and cell viability was determined by removing 100 µL of culture medium and adding 100 µL of Cell-Titer Glo viability reagent. The mixtures were incubated for 10 minutes at 25 °C, and the luminescence signal was quantified on an Envision luminescence plate reader.

HCV 1b Replicon Huh-7 Antiviral and Cytotoxicity Assay

For EC₅₀ and CC₅₀ determinations, compounds were serially diluted in ten steps of 1:3 dilutions in 384-well plates. All serial dilutions were performed in four replicates per compound within the same 384-well plate. An HCV protease inhibitor ITMN-191 at 100 µM was added as a control of 100% inhibition of HCV replication while puromycin at 10 mM was included as a

control of 100% cytotoxicity. To each well of a black polystyrene 384-well plate (Greiner Bio-one, Monroe, NC), 90 μ L of cell culture medium (without Geneticin) containing 2000 suspended HCV replicon cells was added with a Biotek μ Flow workstation. For compound transfer into cell culture plates, 0.4 μ L of compound solution from the compound serial dilution plate was transferred to the cell culture plate on a Biomek FX workstation. The DMSO concentration in the final assay wells was 0.44%. The plates were incubated for 3 days at 37 °C with 5% CO₂ and 85% humidity. The HCV replicon assay was a multiplex assay, able to assess both cytotoxicity and antireplicon activity from the same well. The CC₅₀ assay was performed first. The media in the 384-well cell culture plate was aspirated, and the wells were washed four times with 100 μ L of PBS each, using a Biotek ELX405 plate washer. A volume of 50 μ L of a solution containing 400 nM calcein AM (Anaspec, Fremont, CA) in 1 \times PBS was added to each well of the plate with a Biotek μ Flow workstation. The plate was incubated for 30 min at room temperature before the fluorescence signal (excitation 490 nm, emission 520 nm) was measured with a Perkin-Elmer Envision plate reader. The EC₅₀ assay was performed in the same wells as the CC₅₀ assay. The calcein-PBS solution in the 384-well cell culture plate was aspirated with a Biotek ELX405 plate washer. A volume of 20 μ L of Dual-Glo luciferase buffer (Promega, Madison, WI) was added to each well of the plate with a Biotek μ Flow Workstation. The plate was incubated for 10 min at room temperature. A volume of 20 μ L of a solution containing a 1:100 mixture of Dual-Glo Stop & Glo substrate (Promega, Madison, WI) and Dual-Glo Stop & Glo buffer (Promega, Madison, WI) was added to each well of the plate with a Biotek μ Flow Workstation. The plate was then incubated at room temperature for 10 min before the luminescence signal was measured with a Perkin-Elmer Envision Plate Reader.

Cytotoxicity Assays

HEp-2 (1.5×10^3 cells/well) and MT-4 (2×10^3 cells/well) cells were plated in 384-well plates and incubated with the appropriate medium containing 3-fold serially diluted compound ranging from 15 nM to 100,000 nM. Cells were cultured for 4-5 days at 37 °C. Following the incubation, the cells were allowed to equilibrate to 25 °C, and cell viability was determined by adding Cell-Titer Glo viability reagent. The mixture was incubated for 10 minutes, and the luminescence signal was quantified using an Envision plate reader. Cell lines were not authenticated and were not tested for mycoplasma as part of routine use in cytotoxicity assays.

Human Hepatic S9 and Plasma Stability.

The compounds were incubated at 2 μ M in human hepatic S9 fractions (obtained from In Vitro Technologies, Baltimore, MD) for 90 min at 37 °C in the presence of NADPH and UDPGA (phase I and phase II cofactor, Sigma-Aldrich). At specified time points following compound addition, samples were quenched with nine volumes of an aqueous solution containing internal standard, 50% acetonitrile, and 25% methanol. Sample plates were centrifuged at 3000g for 30 min, and 10 μ L of the resulting solution was analyzed by LC/MS/MS. Data (sample to internal standard peak area ratio) were plotted on a semi log scale and fitted using an exponential fit. Assuming first-order kinetics, the half-life and rate of metabolism were determined. Predicted hepatic extraction was calculated from the half-life by reported methods using the well-stirred model for hepatic clearance. For blood plasma stability, compounds were incubated at 2 μ M in human plasma samples for up to 4 h at 37 °C. At the desired time points, an aliquot from the incubation was quenched by adding 9 volumes of 100% acetonitrile supplemented with internal standard. Following the last collection, the samples were centrifuged at $3,000 \times g$ for 30 min and the supernatants were transferred to a new plate containing an equal volume of water for analysis by LC/MS/MS. The data (analyte-to-internal standard peak area ratio) were plotted on a semi-log scale and fitted using an exponential fit. The half-life ($t_{1/2}$) was determined assuming first-order kinetics.

LC/MS/MS Instrumentation

Liquid chromatography was performed using an Agilent 1200-series quaternary pump system (Agilent Technologies, Santa Clara, CA) with a 2 μ m 20 \times 2.1 mm Mercury RP C18 (Phenomenex, Torrance, CA). A HPLC system was coupled to a Quattro Premier triple-quadrupole mass spectrometer (Waters, Milford, MA). Mass spectrometry was performed in positive-ion mode and multiple reaction monitoring modes using a Quattro Premier (Waters, Milford, MA). The test compound was eluted with a mobile phase consisting of 0.2% formic acid and a linear gradient from 0 to 95% acetonitrile over 2 min.

log D Measurement

A solution of test compound in DMSO (2 μ L of 10 mM) was added into a 96-well plate containing 198 μ L of 1:1 acetonitrile/water. The sample plate was shaken for 30 min, and 10 μ L

of the resulting solution was analyzed by HPLC/UV. The instrumentation used was an Alliance 2795 HPLC coupled with a photodiode array detector 2996 (Waters, Milford, MA) using a Waters XTerra 3.5 μm 4.6 mm \times 50 mm C18 column. The mobile phase consisted of solvent A (20 mM ammonium acetate aqueous solution) and solvent B (100% acetonitrile). Elution was performed using a linear gradient of solvent B from 0% to 100% in 8 min. The log D value was calculated using the retention time of test compound compared to the reference compounds. The range of log D values for reference compounds is approximately between 0.3 and 5.7.

Biochemical Assays

All natural deoxynucleoside triphosphates (dNTPs) and nucleoside triphosphates (NTPs) were from GE Healthcare (Piscataway, NJ). The [α - ^{33}P]dNTPs and [α - ^{33}P]NTPs were purchased from PerkinElmer (Waltham, MA). All of the biochemical assays used radiolabeled dNTP or NTP to track DNA or RNA product formation. The products were analyzed using affinity filter-binding or electrophoresis systems and quantified using a Typhoon Trio imager and ImageQuant TL software (GE Healthcare). All concentrations refer to the final concentrations unless mentioned otherwise. Product formation in the presence of the inhibitors was expressed as a percentage of the product in water-treated controls (defined as 100%). The IC_{50} was defined as the concentration at which there was a 50% decrease in product formation. The data were analyzed using GraphPad Prism 5.0. IC_{50} s were calculated as an average of at least three independent experiments. RSV ribonucleoprotein (RNP) complexes were prepared according to a method modified from Mason *et al.*⁵ The recombinant human mitochondrial RNA polymerase (POLRMT) was purchased from Enzymax. RNA polymerase II was purchased as part of the “HeLaScribe[®] Nuclear Extract *in vitro* Transcription System” kit from Promega. Recombinant human DNA polymerases α and β were gifts from Robert Kuchta at the University of Colorado and Zucui Suo at the Ohio State University, respectively. Recombinant human DNA polymerase γ (including both the large subunit and the small subunit) was cloned, overexpressed, and purified based on published methods.^{6,7}

RSV A2 Polymerase Inhibition Assay

Transcription reactions contained 25 μg of crude RSV RNP complexes in 30 μL of reaction buffer (50 mM TRIS-acetate [pH 8.0], 120 mM potassium acetate, 5% glycerol, 4.5 mM MgCl_2 ,

3 mM DTT, 2 mM EGTA, 50 µg/mL BSA, 2.5 U RNasin, 20 µM ATP, 100 µM GTP, 100 µM UTP, 100 µM CTP, and 1.5 µCi [α -³²P]ATP [3,000 Ci/mmol]). The radiolabeled nucleotide used in the transcription assay was selected to match the nucleotide analog being evaluated for inhibition of RSV RNP transcription. To determine whether nucleotide analogs inhibited RSV RNP transcription, compounds were added using a 6-step serial dilution in 5-fold increments. After a 90-minute incubation at 30 °C, the RNP reactions were stopped with 350 µL of Qiagen RLT lysis buffer, and the RNA was purified using a Qiagen RNeasy 96 kit. Purified RNA was denatured in RNA sample loading buffer at 65 °C for 10 minutes and run on a 1.2% agarose/MOPS gel containing 2M formaldehyde. The agarose gel was dried, exposed to a Storm phosphorimaging screen, and developed using a Storm phosphorimager.

HCV NS5B Inhibition Assay

A reaction mixture containing 50 mM Tris-HCl (pH 7.5), 10 mM KCl, 1 mM dithiothreitol (DTT), 0.1 mg/ml bovine serum albumin (BSA), 0.2 U/µl RNasin Plus RNase inhibitor (Promega), 4 ng/µl sshRNA, 5 mM MgCl₂, and 70 to 150 nM wild-type HCV NS5B was preincubated with NTP analog for 5 min at room temperature. The reaction was initiated by adding a mixture containing 2.5 µM ATP, 2.5 µM CTP, 2.5 µM UTP, 1.25 µM GTP, and 0.06 µCi/µl of [α -³³P]GTP (3,000 mCi/mol). The reactions were allowed to proceed for 90 min at 30 °C. After 90 min, 10 µl of the reaction mixture was spotted on DE81 anion exchange paper (Whatman, United Kingdom), which was then washed with 3× Na₂HPO₄ (125 mM [pH 9]), 1× water, and 1× ethyl alcohol (EtOH). The filter paper was air-dried and exposed to the phosphorimager screen, and the amount of synthesized RNA was quantified as described earlier.

Inhibition of Human DNA and RNA Polymerases

All reaction mixtures contained 50 mM Tris-HCl buffer (pH 8.0), 0.2 mg/ml BSA, 2 mM DTT, 0.05 mg/ml activated fish sperm DNA, 10 mM MgCl₂, 1.3 µCi [α -³³P]dTTP (3,000 Ci/mmol), and 2 µM each of dATP, dGTP, and TTP. The optimal enzyme concentrations were chosen to be in the linear range of enzyme concentration ([E]) versus activity, and the reaction time was selected to ensure that 10% of the substrate was consumed. All reactions were run at 37 °C. The amounts of enzyme used in each assay were 160 nM and 30 nM for polymerase α and β , respectively. For polymerase γ holoenzyme, 1.2 nM large catalytic subunit and 3.6 nM small

accessory subunit were used in the assay. The incubation times were 30 min, 10 min, and 60 min for polymerases α , β , and γ , respectively. The reactions were started by adding a mixture of the abovementioned natural NTPs and MgCl_2 into a preincubated mixture containing enzyme and inhibitors. At the end of the incubation, 5 μl of the reaction mixture was removed and spotted on DE81 anion exchange paper (Whatman, United Kingdom), which was washed with $3\times \text{Na}_2\text{HPO}_4$ (125 mM [pH 9]), $1\times$ water, and $1\times$ EtOH. The filter paper was air-dried and exposed to the phosphorimager screen prior to quantification and analysis. Human RNA polymerase II reactions were conducted by preincubating 7.5 μl $1\times$ transcription buffer (20 mM HEPES [pH 7.2 to 7.5], 100mM KCl, 0.2mM EDTA, 0.5mM DTT, 20% glycerol), 3mM MgCl_2 , 100 ng cytomegalovirus (CMV)-positive control DNA (Promega), a mixture of natural NTPs, and various concentrations of the inhibitors at 30 °C for 5 min. The mixture of four natural NTPs contained 5 μCi of the competing NTP, with the concentration set at the K_m , and 400 μM the three noncompeting NTPs. The reaction was started by adding 3.5 μl of HelaExtract to a final 25- μl reaction mixture. After 1 h incubation at 30°C, the polymerase reaction was stopped by adding 10.6 μl of proteinase K mixture, which contained final concentrations of 2.5 $\mu\text{g}/\mu\text{l}$ proteinase K (New England BioLabs), 5% SDS, and 25mM EDTA. After incubation at 37 °C for 3 to 12 h, 10 μl of the reaction mixture was mixed with 10 μl of the loading dye (98% formamide, 0.1% xylene cyanol, and 0.1% bromophenol blue), heated at 75 °C for 5 min, and loaded onto a 6% polyacrylamide gel (8 M urea). The gel was dried for 45 min at 70 °C and the full-length product (363 nt runoff RNA) was quantified. The inhibition of mitochondrial RNA polymerase (POLRMT) was evaluated using 20nMPOLRMT preincubated with 20nMtemplate plasmid (pUC18-LSP) containing POLRMT light-strand promoter region and mitochondrial transcription factor A (mtTFA) (100 nM) and mt-TFB2 (20 nM) in buffer containing 10mM HEPES (pH 7.5), 20mMNaCl, 10mM DTT, 0.1 mg/ml BSA, and 10mM MgCl_2 . The reactions were heated to 32 °C and initiated by adding 2.5 μM each of the four natural NTPs and 1.5 μCi of [^{33}P]GTP. After incubation for 30 min at 32 °C, the reactions were spotted on DE81 paper before being processed for quantification.

Single Nucleotide Incorporation by Mitochondrial RNA Polymerase

A mixture of MTCN buffer (50 mM MES, 25 mM Tris-HCl, 25 mM CAPS, and 50 mM NaCl, pH 7.5), 200 nM 5'- ^{32}P -R12/D18, 10mM MgCl_2 , 1 mM DTT, and 376 nM POLRMT was

preincubated at 30 °C for 1 min. The reaction was started by addition of 500 μM (final) natural NTP or NTP analogs. At selected time points, the reaction mixture was removed and quenched with gel loading buffer containing 100 mM EDTA, 80% formamide, and bromophenol blue, and heated at 65 °C for 5 min. The samples were run on a 20% polyacrylamide gel (8 M urea), and the product formation was quantified using Typhoon Trio Imager and Image Quant TL Software (GE Healthcare, Piscataway, NJ). The rate of single nucleotide incorporation by mt RNA pol was calculated by fitting the product formation using the single exponential equation: $[R13] = A(1 - e^{-kt})$, where $[R13]$ represents the amount (in nM) of the elongated product formed, t represents the reaction time, k represents the observed rate, and A represents the amplitude of the exponential.

Single Nucleotide Incorporation by Mitochondrial DNA Polymerase γ

An annealed ^{32}P labeled primer-template D19/D36, 1.2 nM DNA Pol γ large subunit, and 3.4 nM Pol γ accessory subunit are preincubated on ice for 5 minutes and added to reaction mixture containing 50 mM Tris-Cl (pH 8.0), 2 mM DTT, 0.2 mg/mL BSA, 200 nM D19/D36 mer and 10 mM MgCl_2 . Reactions are heated to 37 °C and initiated by addition of 50 μM (final) natural dNTP or analog, plus 50 μM of a natural dNTP that allows the primer to regenerate after 3'-excision by the exonuclease activity of the enzyme. At 0, 5, 10, 30, 60, and 90 min, 10 μL of the reaction mixture is removed and quenched with 10 μL of a gel loading buffer containing 100 mM EDTA, 80% formamide and bromophenol blue, and heated at 65 °C for 5 minutes. The samples are run on a 20% polyacrylamide gel (8 M urea) and the gel is exposed to a phosphorimager screen. The substrate and the incorporation products, D19 and D20-28, are quantified using a Typhoon Trio Imager and Image Quant TL Software. The rate nucleotide incorporation is calculated in Prism by fitting the product formation using the single exponential equation: $[D20] = A(1 - e^{-kt})$, where $[D20]$ represents the amount (in nM) of the elongated product formed, t represents the reaction time, k represents the observed rate, and A represents the amplitude of the exponential. Analog incorporation rates are calculated as % incorporation relative to natural dNTP.

Molecular modeling

Comment [DS2]: Need Revisions With Jason Perry's Additions

A homology model of RSVA2 and EBOV polymerases were built using the HIV-RT X-ray crystal structure (PDB:1RTD). (Schrödinger Release 2015-1: Prime, version 3.9, Schrödinger, LLC, New York, NY, 2015, default settings with subsequent rigid body minimization and side chain optimization. Loop insertions not in 1RTD of greater than 10 amino acids were not built).

Preparation of Small Molecule Compounds

The synthesis and characterization data for the following compounds have been previously described: **4**⁸⁻¹³, **4b**^{10,11,14,15}, **7**^{9,16}, **8**^{8,11,12}, **9**^{8,11,12}, **10**¹⁷, **11**^{18,19}, **11a**^{18,19}, **12**^{20,11}, **13**^{12,21,22}, **13a**^{12,21,22}, **13b**^{12,21,22}, **4-TP**¹⁰. The synthesis and characterization for the following intermediates have been previously described: **22g**²³, **22h**²⁴, **22j** (single Sp isomer)^{21,22}, **22m**²⁴, **22n**²⁵. The second generation synthesis and characterization of **4**, **4b**, **21** and **22b** has been described previously.¹⁰

Comment [RM3]: Compounds to be added 13-TP; 22a, 18a, 18b

2-Ethylbutyl (((((2R,3S,4R,5S)-5-(4-aminopyrrolo[2,1-f][1,2,4]triazin-7-yl)-5-ethynyl-3,4-dihydroxytetrahydrofuran-2-yl)methoxy)(phenoxy)phosphoryl)-L-alaninate (**9a**)

To a solution of compound **9** (15 mg, 0.053 mmol) in anhydrous THF (3 mL) was added *t*-BuMgCl (1M in THF, 79 µL, 0.079 mmol) at rt under a nitrogen atmosphere. After 20 min, a solution of **19** (47 mg, 0.106 mmol) in anhydrous THF (3 mL) was added and the resulting mixture was warmed to 50 °C. After 12 h, the reaction mixture was concentrated under reduced pressure and the crude residue was purified by reverse phase preparatory HPLC to afford compound **9a** (6.6 mg, 21%, ~1:1 diastereomeric mixture at phosphorus). HRMS (*m/z*): [M]⁺ calcd for C₂₈H₃₆N₅O₈P, 602.2307; found, 602.2380. HPLC: t_R = 5.572 min, 5.622 min.

(2S)-2-ethylbutyl 2-((((((2R,3S,4R,5R)-5-(4-aminopyrrolo[2,1-f][1,2,4]triazin-7-yl)-5-cyano-3,4-dihydroxytetrahydrofuran-2-yl)methoxy)(phenoxy)phosphoryl)amino) propanoate (**4a**)

To a solution of Compound **22a** (1.08 g, 2.4 mmol) in anhydrous DMF (9 mL) at rt was added **4** (350 mg, 1.2 mmol) in one portion. A solution of *t*-butylmagnesium chloride in THF (1M, 1.8 mL, 1.8 mmol) was then added to the reaction dropwise over about 10 minutes. The reaction was stirred for about 2 h, at which point the reaction mixture was diluted with ethyl acetate (50

mL) and washed with saturated aqueous sodium bicarbonate solution (3 x 15 mL) followed by saturated aqueous sodium chloride solution (15 mL). The organic layer was dried over anhydrous sodium sulfate and concentrated under reduced pressure. The resulting oil was purified with silica gel column chromatography (eluent: 0-10% methanol in dichloromethane) to **4a** (311 mg, 43%, 1 : 0.4 diastereomeric mixture at phosphorus). ¹H NMR (400 MHz, methanol-*d*₄) δ 7.85 (m, 1H), 7.34 – 7.23 (m, 2H), 7.21 – 7.09 (m, 3H), 6.94 – 6.84 (m, 2H), 4.78 (d, *J* = 5.4 Hz, 1H), 4.46 – 4.33 (m, 2H), 4.33 – 4.24 (m, 1H), 4.18 (m, 1H), 4.05 – 3.80 (m, 3H), 1.52 – 1.39 (m, 1H), 1.38 – 1.20 (m, 7H), 0.85 (m, 6H). ³¹P NMR (162 MHz, methanol-*d*₄) δ 3.71, 3.65. MS *m/z* 603.1 [M+1].

Separation of the *Sp* and *Rp* Diastereomers of **4a**

4a was dissolved in acetonitrile. The resulting solution was loaded onto Lux Cellulose-2 chiral column, equilibrated in acetonitrile, and eluted with isocratic acetonitrile/methanol (95:5 vol/vol). The first eluting compound was the *Rp* diastereomer **4c**, and the second eluting compound was the *Sp* diastereomer **4b**.

(2*S*)-ethyl 2-(((4-nitrophenoxy)(phenoxy)phosphoryl)amino)-3-phenylpropanoate (**22d**).

[0001] (*S*)-ethyl 2-amino-3-phenylpropanoate hydrochloride (1.01 g, 4.41 mmol) was dissolved in dichloromethane (50 mL). This solution was cooled to about 0 °C and PhOP(O)Cl₂ (0.656 mL, 4.41 mmol) was added, followed by the slow addition of Et₃N (1.62 mL, 11.5 mmol) over 5 min. The cold bath was removed and the reaction was allowed to warm to rt and stir over a period of 80 min. *p*-NO₂PhOH (0.583 g, 4.19 mmol) was added, followed by more Et₃N (0.3 mL, 2.1 mmol). The reaction progress was monitored by LC/MS. Upon completion of the reaction, it was diluted with Et₂O, and the resulting solids were removed by filtration. The filtrate was concentrated the crude residue was purified by silica gel column chromatography (eluent: 0-55% ethyl acetate in hexanes) to afford compound **22d** (1.25 g, 60%, as a mixture of diastereomers). ¹H NMR (400 MHz, methanol-*d*₄) δ 8.17 (m, 2H), 7.33 (m, 2H), 7.09-7.25 (m, 10H), 4.17 (m, 1H), 4.07 (m, 2H), 3.08 (m, 1H), 2.84 (m, 1H), 1.14 (m, 3H). ³¹P NMR (162 MHz, DMSO-*d*₆) δ -1.479 (s), -1.719 (s). MS *m/z* = 471.01 [M+1].

(2*S*)-ethyl 3-methyl-2-(((4-nitrophenoxy)(phenoxy)phosphoryl)amino) butanoate (**22e**).

(*S*)-Ethyl 2-amino-3-methylbutanoate (0.351 g, 1.93 mmol) was dissolved in CH₂Cl₂ (17 mL). This solution was cooled in an ice bath and PhOP(O)Cl₂ (0.287 mL, 1.93 mmol) was added, followed by the slow addition of Et₃N (1.62 mL, 11.4 mmol) over about 5 min. The cold bath was removed and the reaction was allowed to warm to rt and stir over a period of 1 h. *p*-NO₂PhOH (0.255 g, 1.83 mmol) was added, and the reaction progress was monitored by LC/MS. Upon completion of the reaction, the mixture was diluted with Et₂O, and the resulting solids were removed by filtration. The filtrate was concentrated and the crude residue was purified by silica gel column chromatography (eluent: 0-55% ethyl acetate in hexanes) to afford compound **22e** (0.642 g, 79%, as a mixture of diastereomers). ¹H NMR (400 MHz, DMSO-*d*₆) δ 8.30 (d, *J* = 9.2 Hz, 2H), 7.48 (t, *J* = 9.6 Hz, 2H), 7.40 (t, *J* = 7.8 Hz, 2H), 7.20-7.27 (m, 3H), 6.60 (q, *J* = 11.6 Hz, 1H), 4.01 (m, 2H), 3.61 (m, 1H), 1.93 (m, 1H), 1.11 (m, 3H), 0.79 (m, 6H). ³¹P NMR (162 MHz, DMSO-*d*₆) δ -0.342 (s), -0.578 (s). MS *m/z* = 422.9 [M+1].

Ethyl 2-methyl-2-(((4-nitrophenoxy)(phenoxy)phosphoryl)amino)propanoate (22f).

Phenyl dichlorophosphate (0.97 mL, 6.50 mmol) and ethyl 2-amino-2-methylpropanoate hydrochloride (1.09 g, 6.50 mmol) were dissolved in CH₂Cl₂ (50 mL). The reaction mixture was cooled to about 0 °C and Et₃N (1.75 mL, 12.5 mmol) was slowly added. The reaction mixture was allowed to warm to rt. After 2 h, *p*-nitrophenol (0.860 g, 6.17 mmol) was added followed by the Et₃N (0.87 g, 7.69 mmol). After about 2 h, the reaction was determined to be complete by LCMS. The reaction was diluted with Et₂O and the precipitate was removed by filtration. The resulting filtrate was concentrated under reduced pressure and the crude residue was purified by silica gel chromatography (eluent: 0-50% ethyl acetate in hexanes) to afford compound **22f** ((1.79 g, 68%). ¹H NMR (400 MHz, DMSO-*d*₆) δ 8.37 – 8.21 (m, 2H), 7.55 – 7.44 (m, 2H), 7.43 – 7.33 (m, 2H), 7.30 – 7.09 (m, 3H), 6.57 (d, *J* = 10.1 Hz, 1H), 3.99 (q, *J* = 7.1 Hz, 2H), 1.39 (s, 6H), 1.08 (t, *J* = 7.1 Hz, 3H). ³¹P NMR (162 MHz, DMSO-*d*₆) δ -2.87. MS *m/z* = 408.97 [M+1].

(2*S*)-cyclobutyl 2-(((4-nitrophenoxy)(phenoxy)phosphoryl)amino)propanoate (22i).

Phenyl dichlorophosphate (1.49 mL, 10 mmol) was dissolved in 10 mL of anhydrous dichloromethane and stirred under atmosphere nitrogen in an ice bath. Cyclobutyl-L-alinate hydrochloride (0.9 g, 5 mmol) was added in one portion. Triethylamine (765 μL, 5.5 mmol) was then added dropwise. The reaction mixture was stirred for about 1 h, and triethylamine (765 μL,

5.50 mmol) was added dropwise and the reaction was stirred for about 45 min. *p*-Nitrophenol (1.25 g, 9 mmol) was added in one portion and stirred for about 30 min. Triethylamine (765 μ L, 5.5 mmol) was added and the reaction mixture was stirred for about 2 h. Additional *p*-nitrophenol (1.25 g, 9 mmol) and triethylamine (765 μ L, 5.50 mmol) were then added, and the reaction was stirred for another 2 h. The reaction mixture was concentrated under reduced pressure, and the resulting crude residue was diluted with ethyl acetate and washed twice with 5% aqueous citric acid solution, and once with saturated aqueous sodium chloride solution. The organic layer was then dried over anhydrous sodium sulfate and concentrated under reduced pressure. The crude residue was purified with silica gel column chromatography (eluent: 0-50% ethyl acetate in hexanes) to afford compound **22i** (1.48 g, 70% yield as a mixture of diastereomers). ^1H NMR (400 MHz, methanol- d_4) δ 8.33 – 8.23 (m, 2H), 7.52 – 7.33 (m, 4H), 7.33 – 7.17 (m, 3H), 4.96 – 4.85 (m, 1H), 4.07 – 3.96 (m, 1H), 2.27 (m, 2H), 2.07 – 1.91 (m, 2H), 1.83 – 1.70 (m, 1H), 1.70 – 1.55 (m, 1H), 1.32 (m, 3H). ^{31}P NMR (162 MHz, methanol- d_4) δ -1.36, -1.59. MS m/z = 420.9 [M+1].

***tert*-Butyl ((4-nitrophenoxy)(phenoxy)phosphoryl)-L-alaninate (22k).**

A suspension of L-Alanine *t*-butylester hydrochloride (475 mg, 2.62 mmol) was suspended in methylene chloride (10 mL), and phenyl dichlorophosphate (0.39 mL, 2.62 mmol) was added rapidly at -78°C . A solution of triethylamine (0.72 mL, 5.24 mmol) in methylene chloride (1.5 mL) was then added over 60 min at -78°C and the resulting mixture was stirred at room temperature for 3 h. The reaction mixture was cooled to 0°C and 4-nitrophenol (364 mg, 2.62 mmol) was added in one portion. Then triethylamine (0.36 mL, 2.62 mmol) was added over 60 min and the reaction mixture was stirred at rt. After 3 h, the reaction mixture was diluted with ethyl acetate, washed with saturate aqueous sodium carbonate solution (3 \times), dried over sodium sulfate, and concentrated under reduced pressure. The crude residue was purified by silica gel column chromatography (eluent: 0-35% ethyl acetate in hexanes) to afford **22k** (2.3 g, 79%). ^1H NMR (400 MHz, chloroform- d_1) δ 8.30 – 8.18 (m, 2H), 7.46 – 7.29 (m, 4H), 7.31 – 7.14 (m, 3H), 4.01 (tt, J = 8.5, 6.5 Hz, 1H), 3.93 – 3.70 (m, 1H), 1.43 (s, 9H), 1.37 (dd, J = 7.0, 2.0 Hz, 3H). ^{31}P NMR (162 MHz, chloroform- d_1) δ -2.85. MS m/z = 844 [2M+1].

Cyclobutylmethyl ((4-nitrophenoxy)(phenoxy)phosphoryl)-L-alaninate (22l).

To a suspension of L-alanine cyclobutylmethyl ester hydrochloride (1.2 g, 7.2 mmol) in methylene chloride (10 mL) was added phenyl dichlorophosphate (1.07 mL, 7.16 mmol) rapidly at $-78\text{ }^{\circ}\text{C}$. Triethylamine (2.0 mL, 14.0 mmol) was added over 60 min at $-78\text{ }^{\circ}\text{C}$ and the resulting mixture was stirred at rt for 3 h. The reaction mixture warmed to $0\text{ }^{\circ}\text{C}$ and 4-nitrophenol (996 mg, 7.16 mmol) was added in one portion. Then triethylamine (1.0 mL, 7.2 mmol) was added over 60 min, and the reaction mixture was then stirred at room temperature. After 3 h, the reaction mixture was diluted with ethyl acetate, washed with saturate aqueous sodium carbonate solution (3 \times), dried over sodium sulfate, and concentrated under reduced pressure. The crude residue was purified by silica gel column chromatography (eluent: 0-35% ethyl acetate in hexanes) to afford **221** (2.3 g, 85%). ^1H NMR (400 MHz, chloroform- d_1) δ 8.30 – 8.16 (m, 2H), 7.45 – 7.30 (m, 4H), 7.30 – 7.18 (m, 3H), 4.23 – 4.02 (m, 3H), 3.94 – 3.84 (m, 1H), 2.58 (m, 1H), 2.03 (m, 2H), 1.98 – 1.81 (m, 2H), 1.73 (m, 2H), 1.41 (m, 3H). ^{31}P NMR (162 MHz, chloroform- d_1) δ -3.06 , -3.11 . MS m/z = 435 [M+1].

Single Crystal X-ray Diffraction

Single Crystal X-ray Diffraction of Compound 22b

The single crystal X-ray Diffraction of compound **22b** has been described previously.¹⁰ The absolute stereochemistry of compound **22b** is unambiguous. The X-ray crystallographic coordinates and structure factor files for compound **22b** have been deposited in the Cambridge Structural Database (accession number 1445315, <http://www.ccdc.cam.ac.uk/>).

Single Crystal X-ray Diffraction of Compound 4b

The single crystal X-ray diffraction studies were carried out on a Bruker APEX CCD diffractometer equipped with Cu K α radiation ($\lambda = 1.54178$). A $0.220 \times 0.080 \times 0.040$ mm colorless needle of **4b** grown from a dichloromethane solution was mounted on a Cryoloop with Paratone oil. Data were collected in a nitrogen gas stream at 100(2) K using ϕ and ω scans. The diffractometer was a Bruker D8 platform equipped with a Nonius FR-591 rotating anode generator and micro-focus optics. Crystal-to-detector distance was 60 mm and exposure time was 5 s/frame using a scan width of 0.5° . Data collection was 97.9% complete to 65.67° in θ . A total of 14875 reflections were collected covering the indices, $-12 \leq h \leq 12$, $-8 \leq k \leq 8$, $-25 \leq l \leq 25$. 5666 reflections were found to be symmetry independent, with a R_{int} of 0.0864. Indexing and unit cell refinement indicated a primitive, monoclinic lattice. The space group was found to be $P2_1$. The data were integrated using the Bruker SAINT software program and scaled using the SADABS software program. Solution by direct methods (SHELXS) produced a complete phasing model consistent with the proposed structure. All nonhydrogen atoms were refined anisotropically by full-matrix least-squares (SHELXL-97). All hydrogen atoms were placed using a riding model. Their positions were constrained relative to their parent atom using the appropriate HFIX command in SHELXL-97. The overall quality of this structure is compromised by weak and broad diffraction that may have resulted from a partial desolvation of the crystals. The absolute stereochemistry is about 95% reliable. The X-ray crystallographic coordinates and structure factor files for compound **4b** have been deposited in the Cambridge Structural Database (accession number XXXXXX, <http://www.ccdc.cam.ac.uk/>).

Comment [DS4]: Submit to Database

Figure S1. Thermal ellipsoid representation of compound **4b**.

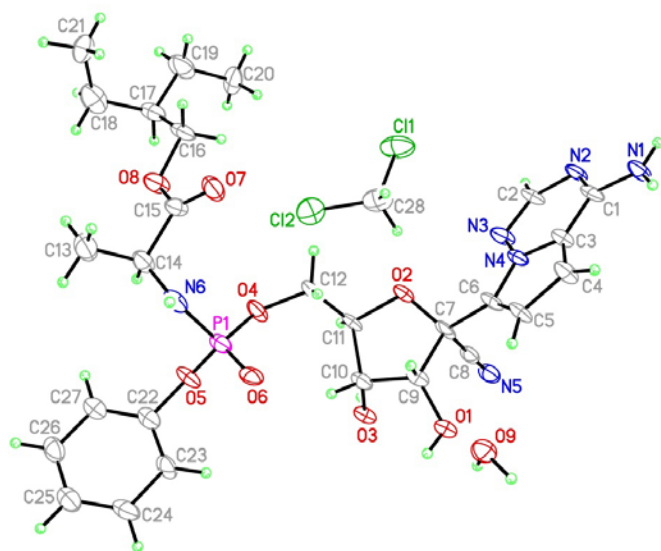


Table S1. Crystal data and structure refinement for compound **4b**.

Empirical formula	C ₂₇ H ₃₅ Cl ₂ N ₆ O ₉ P	
Formula weight	689.48	
Temperature	100(2) K	
Wavelength	1.54178 Å	
Crystal system	Monoclinic	
Space group	<i>P</i> 2 ₁	
Unit cell dimensions	<i>a</i> = 10.5800(4) Å	$\alpha = 90^\circ$
	<i>b</i> = 7.4526(4) Å	$\beta = 92.500(3)^\circ$
	<i>c</i> = 21.5691(12) Å	$\gamma = 90^\circ$
Volume	1699.07(15) Å ³	
<i>Z</i>	2	
Density (calculated)	1.348 Mg/m ³	
Absorption coefficient	2.658 mm ⁻¹	
<i>F</i> (000)	720	
Crystal size	0.22 × 0.08 × 0.04 mm ³	
Theta range for data collection	4.103 to 65.670°.	
Index ranges	-12 ≤ <i>h</i> ≤ 12, -8 ≤ <i>k</i> ≤ 8, -25 ≤ <i>l</i> ≤ 25	
Reflections collected	14875	
Independent reflections	5666 [R(int) = 0.0864]	
Completeness to theta = 66.000°	97.9 %	
Absorption correction	Multi-scan	
Refinement method	Full-matrix least-squares on <i>F</i> ²	
Data / restraints / parameters	5666 / 1 / 416	
Goodness-of-fit on <i>F</i> ²	1.352	
Final <i>R</i> indices [<i>I</i> > 2σ(<i>I</i>)]	<i>R</i> 1 = 0.1269, <i>wR</i> 2 = 0.3342	
<i>R</i> indices (all data)	<i>R</i> 1 = 0.1434, <i>wR</i> 2 = 0.3467	
Absolute structure parameter	0.128(18)	
Extinction coefficient	n/a	
Largest diff. peak and hole	1.453 and -0.614 e.Å ⁻³	

References

1. Lohmann, V.; Körner, F.; Koch, J. -O.; Herian, U.; Theilmann, L.; Bartenschlager, R. Replication of Subgenomic Hepatitis C Virus RNAs in a Hepatoma Cell Line. *Science* **1999**, 285, 110-113.
2. Cheng, G.; Chan, K.; Yang, H.; Corsa, A.; Pokrovskii, M.; Paulson, M.; Bahador, G.; Zhong, W.; Delaney, W. IV Selection of Clinically Relevant Protease Inhibitor-Resistant Viruses Using the Genotype 2a Hepatitis C Virus Infection System. *Antimicrob. Agents Chemother.* **2011**, 55, 2197-2205.
3. Uebelhoer, L. S.; Albarino, C. G.; McMullan, L. K.; Chakrabarti, A. K.; Vincent, J. P.; Nichol, S. T.; Towner, J. S. High-Throughput, Luciferase-Based Reverse Genetics Systems for Identifying Inhibitors of Marburg and Ebola Viruses. *Antiviral Res.* **2014**, 106, 86-94.
4. Towner, J. S.; Paragas, J.; Dover, J. E.; Gupta, M.; Goldsmith, C. S.; Huggins, J. W.; Nichol, S. T. Generation of eGFP Expressing Recombinant Zaire Ebolavirus for Analysis of Early Pathogenesis Events and High-Throughput Antiviral Drug Screening. *Virology*, **2005**, 332, 20-27.
5. Mason, S. W.; Lawetz, C.; Gaudette, Y.; Dô, F.; Scouten, E.; Lagacé, L.; Simoneau, B.; Liuzzi, M. Polyadenylation-dependent screening assay for respiratory syncytial virus RNA transcriptase activity and identification of an inhibitor. *Nucleic Acids Res.* **2004**, 32, 4758-4767.
6. Johnson A. A.; Tsai, Y.; Graves, S. W.; Johnson, K. A. Human Mitochondrial DNA Polymerase Holoenzyme: Reconstitution and Characterization. *Biochemistry*, **2000**, 39, 1702-1708.

7. Graves, S. W.; Johnson, A. A.; Johnson, K. A. Expression, Purification, and Initial Kinetic Characterization of the Large Subunit of the Human Mitochondrial DNA Polymerase. *Biochemistry*, **1998**, 37, 6050-6058.
8. Cho, A.; Suanders, O. L.; Butler, T.; Zhang, L.; Xu, J.; Vela, J. E.; Feng, J. Y.; Ray, A. S.; Kim, C. U. Synthesis and Antiviral Activity of a Series of 1'-Substituted 4-aza-7,9-dideazaadenosine C-nucleosides. *Bioorg. Med. Chem. Lett.* **2012**, 22, 2705-2707.
9. Metobo, S. E.; Xu, J.; Saunders, O. L.; Butler, T.; Aktoudianakis, E.; Cho, A.; Kim, C. U. Practical Synthesis of 1'-Substituted Tubercidin C-Nucleoside Analogs. *Tetrahedron Lett.* **2012**, 53, 484-486.
10. Warren, T. K.; Jordan, R.; Lo, M. K.; Ray, A. S.; Mackman, R. L.; Soloveva, V.; Siegel, D.; Perron, M.; Bannister, R.; Hui, H. C.; Larson, N.; Strickley, R.; Wells, J.; Stuthman, K. S.; Van Tongeren, S. A.; Garza, N. L.; Donnelly, G.; Shurtleff, A. C.; Retterer, C. J.; Gharaibeh, D.; Zamani, R.; Kenny, T.; Eaton, B. P.; Grimes, E.; Welch, L. S.; Gomba, L.; Wilhelmsen, C. L.; Nichols, D. K.; Nuss, J. E.; Nagle, E. R.; Kugelman, J. R.; Palacios, G.; Doerffler, E.; Neville, S.; Carra, E.; Clarke, M. O.; Zhang, L.; Lew, W.; Ross, B.; Wang, Q.; Chun, K.; Wolfe, L.; Babusis, D.; Park, Y.; Stray, K. M.; Trancheva, I.; Feng, J. Y.; Barauskas, O.; Xu, Y.; Wong, P.; Braun, M. R.; Flint, M.; McMullan, L. K.; Chen, S. S.; Fearn, R.; Swaminathan, S.; Mayers, D. L.; Spiropoulou, C. F.; Lee, W. A.; Nichol, S. T.; Cihlar, T.; Bavari, S. Therapeutic Efficacy of the Small Molecule GS-5734 Against Ebola Virus in Rhesus Monkeys. *Nature* **2016**, 531, 381-385.
11. Mackman, R. L.; Parrish, J. P.; Ray, A. S.; Theodore, D. A. Methods and Compounds for Treating Paramyxoviridae Virus Infections. U.S. Patent 2011045102 July, 22, 2011.

12. Butler, T.; Cho, A.; Kim, C. U.; Saunders, O. L.; Zhang, L. 1'-Substituted Carba-nucleoside Analogues for Antiviral treatment. U.S. Patent 2009041447 April, 22, 2009.
13. Butler, T.; Cho, A.; Graetz, B. R.; Kim, C. U.; Metobo, S. E.; Saunders, O. L.; Waltman, A. W.; Xu, J.; Zhang, L. Processes and Intermediates for the Preparation of 1'-substituted Carba-nucleoside Analogues. U.S. Patent 20100459508 September, 20, 2010.
14. Axt, S. D.; Badalov, P. R.; Brak, K.; Campagna, S.; Chtchemelinine, A.; Doerffler, E.; Frick, M. M.; Gao, D.; Heumann, L. V.; Hoang, G.; Lew, W.; Milburn, R. R.; Neville, S. T.; Ross, B.; Rueden, E.; Scott, R. W.; Siegel, D.; Stevens, A. C.; Tadeus, C.; Vieira, T.; Waltman, A. W.; Wang, X.; Whitcomb, M. C.; Wolfe, L.; Yu, C.-Y. Methods for the Preparation of Ribosides. U.S. Patent 2015057932, October, 29, 2015.
15. Chun, B. K.; Clarke, M. O. H.; Doerffler, E.; Hui, H. C.; Jordan, R.; Mackman, R. L.; Parrish, J. P.; Ray, A. S.; Siegel, D. Methods for Treating Filoviridae Virus Infections. U.S. Patent 2015057933, October, 29, 2015.
16. Clarke, M. O. H.; Doerffler, E.; Mackman, R. L.; Siegel, D. Pyrrolo[1,2,F][1,2,4] Triazines Useful for Treating Respiratory Syncytial Virus Infections. U.S. Patent 2014064412 November, 6, 2014.
17. Zhen, L.; Guorong, C.; Yuyuan, X. Cyanoribofuranoside Compound and Its Preparing Method. Chinese Patent 01137132 February, 4, 2004.
18. Kirschberg, T. A.; Mish, M.; Squires, N. H.; Zonte, S.; Aktoudianakis, E.; Metobo, S.; Butler, T.; Ju, X.; Cho, A.; Ray, A. S.; Kim, C. U. Synthesis of 1'-C-Cyano Pyrimidine Nucleosides and Characterization as HCV Polymerase Inhibitors. *Nucleosides, Nucleotides and Nucleic Acids*, **2015**, 34, 763-785.

19. Cho, A.; Kim, C. U.; Kirschberg, T. A.; Mish, M. R.; Squires, N. 1'-Substituted Pyrimidine *N*-Nucleoside Analogues for Antiviral Treatment. U.S. Patent 2012033675 April, 13, 2012.
20. Clarke, M. O. H.; Kim, C. U.; Lew, W. 2'-Fluoro Substituted Carba-Nucleoside Analogs for Antiviral Treatment. U.S. Patent 2011051249 September, 12, 2011.
21. Cho, A.; Zhang, L.; Xu, J.; Lee, R.; Butler, T.; Metobo, S.; Aktoudianakis, V.; Lew, W.; Ye, H.; Clarke, M.; Doerffler, E.; Byun, D.; Wang, T.; Babusis, D.; Carey, A. C.; Berman, P.; Sauer D.; Zhong, W.; Rossi, S.; Fenaux, M.; McHutchison, J. G.; Perry, J.; Feng, J.; Ray, A. S.; Kim, C. U. Discovery of the First *C*-nucleoside HCV Polymerase Inhibitor (GS-6620) with Demonstrated Antiviral Response in HCV Infected Patients. *J. Med. Chem.***2014**, 57, 1812-1825.
22. Cho, A.; Wolckenhauer, S. A. Methods for the Preparation of Diastereomerically Pure Phosphoramidate Prodrugs. U.S. Patent 2011044581 July, 19, 2011.
23. Cho, A.; Kim, C. U.; Metobo, S. E.; Ray, A. S. 2'-Fluoro Substituted Carba-Nucleoside Analogues for Antiviral Treatment. U.S. Patent 2010049471 September, 20, 2010.
24. Kalayanov, G.; Pinho, P.; Westerlind, H.; Wikteliuss, D.; Waehling, H. Preparation of Nucleotides as Hepatitis C Polymerase Inhibitors, European Patent 3057976 October, 16, 2014.
25. Du, J. Sofia, M. J. Compounds. U.S. Patent 2011062643 November, 30, 2011.